

PHARMACOGNOSIC DRUG DISCOVERY WITH THE *YERSINIA PESTIS* MEP SYNTHASE
(ISPC), A VALIDATED TARGET FOR THE DEVELOPMENT OF NOVEL ANTIBIOTICS

by

Tyrone M. Dowdy
A Thesis
Submitted to The
Graduate Faculty
of
George Mason University
in Partial Fulfillment of
The Requirements for The Degree
of
Master of Science
Chemistry

Committee:

_____	Dr. Robin Couch, Thesis Director
_____	Dr. Barney Bishop, Committee Member
_____	Dr. John Schreifels, Committee Member
_____	Dr. John Schreifels, Department Chair
_____	Dr. Donna M. Fox Associate Dean, Office of Student Affairs & Special Programs, College of Science
_____	Dr. Peggy Agouris, Dean, College of Science
Date: _____	Fall Semester 2015 George Mason University Fairfax, VA

Pharmacognosic Drug Discovery with the *Yersinia pestis* MEP Synthase (IspC), a Validated
Target for the Development of Novel Antibiotics

A Thesis submitted in partial fulfillment of the requirements for the degree of Master of Science at
George Mason University.

By

Tyrone M. Dowdy
Bachelor of Science
George Mason University, 2000

Director: Dr. Robin Couch, Professor
Department of Chemistry and Biochemistry

Summer Semester 2015
George Mason University
Fairfax, VA



This work is licensed under a [creative commons attribution-noncommercial 3.0 unported license](https://creativecommons.org/licenses/by-nc/3.0/).

DEDICATION

This is dedicated to my family and all who have encouraged me throughout my pursuit of a master degree with the Department of Chemistry and Biochemistry at George Mason University.

ACKNOWLEDGEMENTS

Dr. Robin Couch, for your mentoring on my thesis, experimental design, broad range of metabolomics studies and providing an opportunity to develop analytical research techniques and to contribute to pharmacognosic and infectious disease research.

Dr. John Schreifels, for your participation on my thesis committee and commitment to providing opportunities for chemistry majors to build teaching experience.

Dr. Barney Bishop, for your participation on my thesis committee, academic guidance and for sharing your knowledge on antimicrobial research.

Dr. Paige, for sharing experience in mass spectroscopy analysis, metabolomics and natural product research.

Amanda Haymond, for your work on assays, contributions to this research, collaboration and for sharing exceptional your expertise in enzymology.

Chinchu Johnny, for your work on and valued contribution to the screening of natural products.

Jun Liu, for your work and valued assistance with mass spectrometry.

Richard Young, Jessica Bases, Trishal Patel and Clark Mantooth for your contribution in building the natural product library.

Justin Davis, Allyson Dailey, Steven Roberts and Karl Navarro for your support throughout the project.

The staff at Agilent Technologies Inc. for training and support in the use of LCMS for metabolomic and small molecule research.

TABLE OF CONTENTS

	Page
TABLE OF CONTENTS	v
LIST OF TABLES	vii
LIST OF FIGURES	viii
ABSTRACT	x
INTRODUCTION.....	1
MATERIALS AND METHODS	12
Natural product extraction	12
Purification of recombinant <i>Y. pestis</i> MEP synthase	12
Bacterial growth inhibition assay.....	14
Enzyme kinetic assays	15
Affinity chromatography purification of the inhibitory compound from extract	16
Liquid chromatography and mass spectrometry	16
Hydrolysis of glycoside.....	19
RESULTS AND DISCUSSION	20
Molecular screening of a natural product library	20
Bacterial growth inhibition for <i>Y. pestis</i> with extract 29.....	22
Identification of a novel inhibitor in extract 29	23
Validation of the active inhibitor present in extract 29	31
Validation of the putative identity for the active inhibitor by MS/MS comparative analysis	33
Hydrolysis of potential quercetin glycosides in extract 29	36
Enzyme kinetic characterization of quercetin with <i>Y. pestis</i>	42
Growth inhibition of <i>Y. pestis</i> with quercetin	43
Modality of inhibition by quercetin	45
CONCLUSION	50
APPENDICES	53
APPENDIX A.....	54

APPENDIX B.....	56
APPENDIX C	64
APPENDIX D	66
REFERENCES.....	76
BIOGRAPHY	80

LIST OF TABLES

Tables	Page
Table 1. Potential active compounds identified using tandem MS analysis.	29

LIST OF FIGURES

Figure	Page
Figure 1. The MVA (A) and MEP (B) biosynthetic pathways, leading to the production of isopentenyl pyrophosphate (7) and dimethylallyl pyrophosphate (8).....	4
Figure 2. Fosmidomycin and FR900098.	6
Figure 3: Molecular screening of the natural product extracts.	21
Figure 4. Bacterial growth inhibition assays for <i>Y. pestis</i> with extract 29.....	23
Figure 5. Enzyme kinetic assays with purified analyte using <i>Y. pestis</i> MEP synthase...	24
Figure 6. Chromatograms of the uninhibited control (green) and affinity purified analyte (black) for comparative analysis.	26
Figure 7. Potential active compounds detected in the purified analyte.	30
Figure 8. Comparisons of the inhibitory quality for potential active compounds present in the purified analyte.....	31
Figure 9. MS/MS comparative analyses for quercetin in extract 29 against quercetin commercial-grade standard at collision energies 10 V, 20 V, and 40 V.....	35
Figure 10. Extracted compound chromatogram of quercetin integrated with total ion chromatogram for each of the HCl-treated and untreated extract 29 analytes.	36
Figure 11. Extracted compound chromatogram of quercetin in the HCL-treated and untreated e29 analytes.....	38
Figure 12. Extracted compound chromatogram for the quercetin standard curve integrated with ions of free quercetin detected in the HCl-treated and untreated e29 analytes.	40
Figure 13. Kinetic characterization of quercetin with recombinant MEP synthase.	43
Figure 14. Bacterial growth inhibition assay of <i>Y. pestis</i> with quercetin.....	44
Figure 15. Modality of inhibition for quercetin with respect to NADPH.	47
Figure 16. Modality of inhibition for quercetin with respect to DXP.....	48
Figure 17. Selective molecular screening with <i>Y. pestis</i> bacterial growth inhibition screening.....	55
Figure 18. MS/MS difference spectral analysis for quercetin in extract 29 and quercetin reference.	57
Figure 19. MS/MS difference spectral analysis for extract 29 potential and quercetin 3- β -D-glucoside reference.	58
Figure 20. MS/MS difference spectral analysis for extract 29 potential and quercetin 3-galactoside reference.	59

Figure 21. MS/MS difference spectral analysis for extract 29 potential and quercitrin reference.	60
Figure 22. MS/MS difference spectral analysis for extract 29 potential and epicatechin reference.	61
Figure 23. MS/MS difference spectral analysis for extract 29 potential and epicatechin reference (Negative Mode).....	62
Figure 24. MS/MS difference spectral analysis for extract 29 potential and (±)-catechin reference (Negative Mode).....	63
Figure 25. Standard curve for quercetin reference standards.	65

ABSTRACT

PHARMACOGNOSIC DRUG DISCOVERY WITH THE *YERSINIA PESTIS* MEP SYNTHASE (ISPC), A VALIDATED TARGET FOR THE DEVELOPMENT OF NOVEL ANTIBIOTICS.

Tyrone Dowdy, M.S.

George Mason University, 2014

Thesis Director: Dr. Robin Couch

This thesis explores the role that a renewal in natural product research has in developing countermeasures to emergent antimicrobial resistance. Pharmacognosy, or the study of natural products, was the foundation of the antibiotic era in early 1900s. Due to convergent evolution and competition, organisms have become highly specialized in biosynthesizing secondary metabolites with specific targets in key metabolic pathways of pathogens, parasites, and competitors. Bioprospecting the metabolome of diverse samples of plants, fungi, and bacteria has provided a reliable resource for drug discovery and advancements in biomedical research.

In this project, targeted high-throughput molecular screening has been used to bioprospect natural product extracts containing phytochemicals isolated from a variety of plants harvested from diverse ecosystems. Our aim was to identify novel inhibitors of the enzyme MEP synthase in the non-melavonate pathway for biothreat category A pathogens, such as *Yersinia pestis*. MEP synthase catalyzes the first committed step in the non-melavonate pathway and is the target enzyme in this investigation. The initial high-throughput screen resulted in four hits of interest, the most potent of which was natural extract 29 (e29). Ultracentrifugation affinity chromatography combined with quadrupole time-of-flight tandem mass spectrometry was used to identify the active component (quercetin) within e29. Subsequent enzyme assays confirmed the inhibitory activity of quercetin. Additionally, unlike other known inhibitors of MEP synthase, the

mechanism of inhibition assays revealed that quercetin was an allosteric inhibitor of MEP synthase. Bacterial growth inhibition assays also demonstrated the effectiveness of quercetin as an antibiotic.

INTRODUCTION

In this pharmacognosy investigation, bioprospecting is applied to profile natural product extracts containing secondary metabolites that inhibit a key enzyme determined to be a validated drug target. Raw extracts demonstrating potent inhibition of the drug target may present a potential for the discovery of new classes of antibiotics. In this study, a natural product library was screened with a drug target that was selected on the basis that it is a vital enzyme in an essential metabolic pathway and shares homologs in fulminant pathogens, such as *Yersinia pestis*. The relevance of the target enzyme and related metabolic pathway will be later discussed in greater detail.

Y. pestis is a gram-negative, facultative anaerobic bacterium that can cause zoonotic, vector-borne diseases [1]. The modes of transmission can be either by inhalation of aerosolized bacteria, perforation of the skin by infected animals, or injection from infected insects [2]. Historically, etiological *Y. pestis* has presented a significant threat to global communities due to its virulence and rapid transmittance of the black plague (also known as Black Death) [1, 3]. *Y. pestis* has caused three pandemics throughout history which resulted in high mortality and morbidity rates. *Y. pestis* has been divided into three biovars: *antiqua*, *medievalis*, and *orientalis*. The first pandemic, which resulted from *Y. pestis Antiqua*, occurred between the 5th and 6th century in Asian, Northern African, and the Mediterranean regions [1, 3]. The second pandemic, caused by *Y. pestis medievalis*, occurred throughout Europe during the 14th century [3]. During the 19th century, the third pandemic spread to the major continents due to exposure among mobile military forces and was caused by *Y. pestis orientalis* [1, 3]. *Y. pestis* served as the first biological weapon upon being launched during an assault on a Genoese settlement (located in Caffa, 1346) by the Tartar military who introduced the strategy of catapulting infected cadavers to

siege seaports along the Black Sea [4]. By the same token, Japanese military personnel launched entomological warfare by dispersing canisters of plague-infected vectors onto invading troops during World War II [5, 6]. During the Cold War, there were reports that Soviet military microbiologists were developing means to aerosolize and disperse antibiotic-resistant *Y. pestis* [1, 7]. The Centers for Disease Control (CDC) have classified *Y. pestis* as a Category A biological threat as it can be easily disseminated, presents with high morbidity and mortality, and may potentially pose a threat to national security if deliberately released as a biological weapon [8, 9].

Upon infection, *Y. pestis* utilizes a Type III protein secretion system (T3SS) to open a transmembrane channel and facilitate bacterial-mediated injection of exogenous proteins, such as *Yersinia* outer membrane effector proteins (Yops), into the cytoplasm of host cells, primarily macrophage [11]. This in turn causes cytotoxicity (e.g., YopE), inhibits production of reactive oxygen species (ROS) (e.g., YopH), prevents phagocytosis, and suppresses immune cell signaling and the production of proinflammatory cytokines in macrophage (e.g., YopP and YopM) [1, 3, 10, 11]. The process of secreting effector proteins as well as producing the fraction 1 (F1) antiphagocytic capsule contributes to the overall resistance of *Y. pestis* to innate immune responses of eukaryotic hosts [1]. Moreover, the secretion of the *Y. pestis* bacteriocin known as the pesticin activity (Pst) protein offers additional survival advantages, which can be attributed to narrow spectrum bacteriostatic activity of the Pst toxin against closely related strains [1,12].

The disease can manifest as bubonic plague by targeting white blood cells, septicemic plague by infecting red blood cells, or pneumonic plague upon infecting the lungs [1, 3]. The most fulminant infection occurs at the onset of pneumonic plague, which presents approximately 100% mortality rate for patients that are untreated or unresponsive to treatment [1]. In the event that a pneumonic strain of *Y. pestis* were engineered with drug-resistance genes and deliberately disseminated in a highly populated region, it could pose a significant threat given the potential to be transmitted from person-to-person via the respiratory system.

The isolation of a multidrug-resistant (MDR) *Y. pestis* strain (which is resistant to aminoglycosides, tetracyclines, chloramphenicol, and trimethoprim-sulfamethoxazole), has increased concerns of the biodefense community evermore over availability of and potential for the weaponization of MDR *Y. pestis* strains [2, 13]. Given the rise in drug-resistant bacteria such as methicillin-resistant *Staphylococcus aureus* and the ability to exchange plasmids containing antibiotic resistance genes, there are increasing risks for re-emergence of virulent pathogens such as *Y. pestis* [13, 14]. Given the relative ease by which bacterial cells can naturally acquire antibiotic resistance or can be deliberately engineered with such genetic modifications, the potential for MDR *Y. pestis* to be released as a biological weapon multiplies the threat to military and civilian populations.

The improper use of antibiotics, spread of immunosuppressant diseases, dependency on chemotherapies, and other biological threats have contributed to the widespread problem of MDR diseases [14]. According to a recent report by the CDC [15], approximately 75,000 patients die each year due to nosocomial infections which were unresponsive to antibiotic treatments. A correlation has been found between the spread of immunosuppressant diseases (e.g., HIV), the increasing use of immunosuppressant therapeutic agents (e.g., chemotherapy), and the rise in the morbidity rates for MDR infections [14]. Many of the re-emerging infectious diseases, such as tuberculosis, were global epidemics prior to the nascent availability of antibiotic agents in the early 1900s [14]. The emergence of MDR pathogens, current outbreaks of the Ebola virus, recent domestic attacks with biological agents (e.g., Anthrax), and the risks associated with the weaponization of biological agents underscore the need for novel antimicrobial research [8].

Antibiotic drug discovery includes five main phases: target identification, target validation, lead molecule identification, lead molecule optimization, and preclinical and clinical trials [8]. The use of enzymes as drug targets to screen natural product libraries can lead to advancements in drug discovery. An important focus in this research is the use of a validated drug target, 1-deoxy xylulose 5-phosphate (DXP) reductoisomerase (also referred to as DXR, IspC and MEP

synthase) in the discovery, purification, identification, and validation of novel inhibitors originating from natural products.

2-C-methyl-D-erythritol-4-phosphate (MEP) synthase catalyzes the first committed step in the MEP pathway [8]. The catalytic activity of MEP synthase is required for survival of bacterial pathogens, while it does not have homologs in the mevalonate (MVA) pathway of mammalian hosts, making it an excellent drug target in the discovery and development of novel treatments for the prevention of bacterial diseases [8, 16, 17].

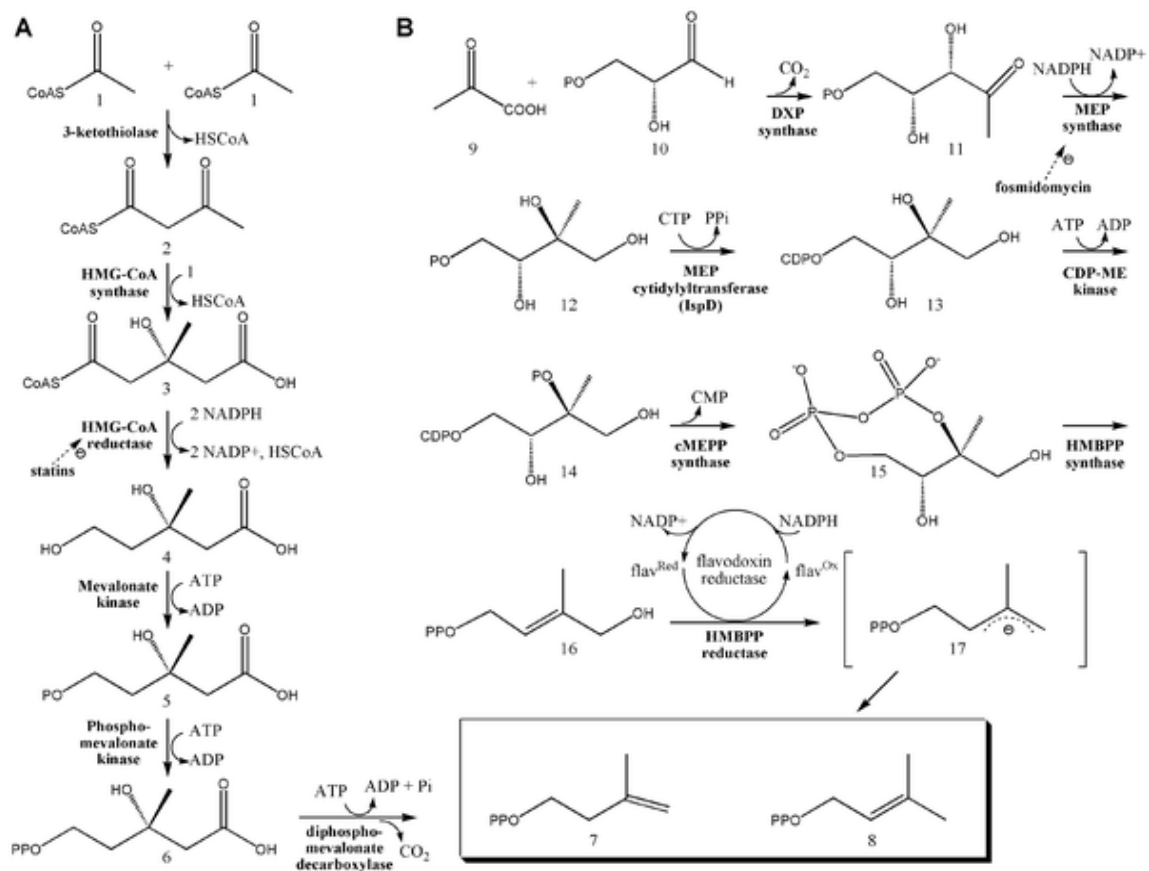


Figure 1. The MVA (A) and MEP (B) biosynthetic pathways, leading to the production of isopentenyl pyrophosphate (7) and dimethylallyl pyrophosphate (8).

Humans and animals depend exclusively on the MVA pathway (Figure 1A) for the biosynthesis of isoprenoid precursors (IPP and DMAPP) [8, 18]. In the MVA pathway, two molecules of acetyl-CoA (1) are condensed by 3-ketothiolase to form acetoacetyl-CoA (2) [19]. 3-hydroxy-3-methylglutaryl-CoA (HMG-CoA) synthase condenses acetoacetyl-CoA with a third acetyl-CoA to form HMG-CoA (3) [19]. HMG-CoA reductase converts HMG-CoA to MVA (4), followed by subsequent phosphorylation by mevalonate kinase and then phosphomevalonate kinase to form mevalonate-5-pyrophosphate (6) [19]. Mevalonate-5-pyrophosphate is decarboxylated by mevalonate-5-pyrophosphate decarboxylase to yield IPP, which is isomerized to form DMAPP by isopentenyl pyrophosphate isomerase [19].

The MEP pathway (Figure 1B), on the other hand, is initiated by the condensation of pyruvate (9) and glyceraldehyde-3-phosphate (10) to 1-deoxy-D-xylulose 5-phosphates (DXP) (11), catalyzed by DXP synthase (DXS). MEP synthase then catalyzes the isomerization of DXP (11) to MEP (12) [8, 20, 21]. 4-diphosphocytidyl-2-C-methylerythritol (CDPME) (13) is formed when the condensation of cytidine triphosphate (CTP) and MEP is catalyzed by MEP-cytidyltransferase (CDPME synthase) [8, 20, 21]. 4-diphosphocytidyl-2-C-methyl-D-erythritol 2-phosphate (CDP-MEP) (14) is formed when CDPME is phosphorylated by CDP-ME kinase [8, 20, 21]. The cyclic intermediate 2-C-methyl-D-erythritol 2,4-cyclodiphosphate (MEcPP) (15) is formed by MEcPP synthase [8, 20]. The cyclopyrophosphate ring is opened to yield (E)-4-hydroxy-3-methyl-but-2-enyl pyrophosphate (HMBPP) (16) by HMBPP synthase [8, 20, 21]. In the final step, HMBPP reductase catalyzes the reduction of HMBPP to produce IPP and DMAPP [8, 20, 21].

Isoprenoids are the building blocks for important biologically active molecules (e.g., sterols, hormones, vitamins, quinones, cholesterol, and terpenoids) essential for metabolism (e.g., cellular respiration, electron transport, signal transduction, membrane modulation, growth regulation, and even antibiotic production) [8, 16, 17, 22, 23, 24]. While the MEP pathway is

utilized by Eubacterium, apicomplexa parasites, and photosynthetic eukaryotes to produce isoprenoid precursors (IPP and DMAPP) [18], humans utilize the MVA pathway (which lacks homologs for MEP pathway enzymes) [8, 18]. Knockout gene studies involving MEP synthase and other enzymes of the MEP pathway have proven that the elimination of the enzyme is lethal for pathogens such as *Mycobacteria tuberculosis*, *Francisella tularensis*, and *Escherichia coli* [8]. Inhibitors that are designed to target the MEP pathway components are not expected to impact the biosynthesis of isoprenoids in human and other mammals [8, 16, 17].

Earlier MEP pathway research demonstrated that natural products such as fosmidomycin and its methylated analog FR900098 (derived from *Streptomyces lavendulae* and *Streptomyces rubellomurinus*, respectively) can provide a valuable resource for the development of potent inhibitors of MEP synthase [16, 17]. FR900098-derived prodrugs, which are analogs synthesized with a lipophilic ester moiety that is expected to undergo enzyme-mediated hydrolytic activation by intracellular esterase, have demonstrated improved anti-tubercular activity by comparison with the parent MEP synthase inhibitor [16, 17].

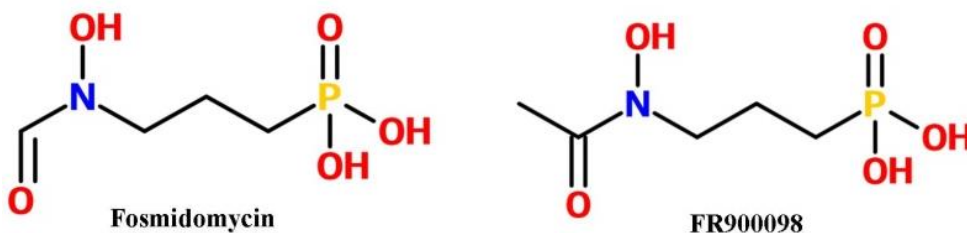


Figure 2. Fosmidomycin and FR900098.

Fosmidomycin and FR900098 (shown in Figure 2) belong to a class of natural products (known as the phosphonates) that depends on the glycerol-3-phosphate transporter (GlpT)

protein to penetrate the bacterial cell membrane [8, 16, 17]. Due to the polar nature of fosmidomycin and FR900098, these antibiotics are unable to enter the bacterial cell without facilitated transport [16, 17]. The resistance of gram-positive bacteria, such as *Mycobacterium tuberculosis* to both fosmidomycin and FR900098 is attributed to the absence of GlpT transporter [8, 16, 17]. In response, the lipophilic prodrug isoforms of FR900098 and fosmidomycin were designed to increase lipophilicity and overcome dependence on GlpT for active transport across the lipid bilayer of bacterial cell membranes [8, 16, 17]. This approach has led to enhancements in the potential for the isoforms of the parent inhibitors to penetrate the cell membrane of virulent pathogens, such as *M. tuberculosis*, *Y. pestis*, *F. tularensis*, *E. coli*, and *Plasmodium falciparum* [16, 17, 23].

Fosmidomycin and FR900098 function as competitive inhibitors by mimicking the substrate DXP and binding in the active site of MEP synthase [16]. Given the emerging threats posed by MDR pathogens, it is critical to invest in research that incorporates alternative approaches (such as pharmacognosy and protein crystallography) to increase the availability of inhibitors that effectively target MEP synthase as well as other enzymes within the MEP pathway. In addition to the development of lipophilic isoforms of FR900098, alternative approaches can increase the potential for the discovery of novel class inhibitors and novel drug binding sites to lead to the development of antibiotics that are more effective than the currently available treatments against infectious diseases.

In addition to bacteria and fungi, plants are highly specialized in producing secondary metabolites that function as alexins (phytochemicals) with biospecificity for enzymes in the metabolic pathways of pathogens, parasites, and competitors [25]. Due to convergent evolution, plants and microbes have developed mechanisms to biosynthesize broad-spectrum natural products (known as phenylpropanoids, alkaloids, and terpenes) that are stored and deployed for chemotactic defense responses to protect against the broad array of microbes that colonize their ecosystems [25]. Even though natural products led the onset of drug discovery in the early

antibiotic era, the identification of lead compounds has been a challenging and time-consuming process [25]. As a result, many drugs currently on the market are derived from natural products that were identified before the 1970s [25]. Two-thirds of the medications available today can be traced back to natural products and related derivatives [26]. Between 1928 and 1944, beta-lactams and aminoglycosides became the first major families of antibiotics that were derived from biosynthesis of natural products by the fungus *Penicillium notatum* and the bacterium *Streptomyces griseus*, respectively [27]. In 2003, beta-lactam-based antibiotics accounted for 65% of the global market [28]. In recent years, the discovery of artemisinin (naturally produced by *Artemisia annua*) led to a turning point in the treatment of MDR malaria [29]. The historical role of natural products in antibiotic development reveals how pharmacognosic research can present robust potential for new treatments against multidrug-resistant pathogens [25]. In planning contingencies to address the looming crisis of drug resistance, investments in natural product research can lead to a broad spectrum of alternative solutions.

The present research utilizes the validated drug target MEP synthase to perform molecular screenings of natural product extracts in order to detect novel inhibitors that can provide potential, effective treatments against MEP pathway-dependent pathogens. This study examines natural product extracts from an in-house library to screen for the presence of active compounds that inhibit the catalytic activity of recombinant MEP synthase inhibitors and to evaluate hit extracts for potential bacteriostatic effect against *Y. pestis* cultures *in vitro*. Then, ultra-high performance liquid chromatography, coupled with quadrupole time-of-flight tandem mass spectrometry (UHPLC QTOF MS/MS) is used to identify the active compounds present in the hit extracts. In addition, enzyme kinetic assays are utilized to quantify the potency of the inhibitor, elucidate the mechanism of inhibition for the identified active compounds, as well as confirm that these characteristics reflect the expectations for inhibitor hits from the natural product library.

EXPERIMENTAL AIMS

1. Prepare a natural product library.

The proprietary, in-house natural product library was developed by organic extraction of the metabolome from biological specimens collected from diverse geological locations.

Bioprospecting a broad array of naturally evolving, uncultivated, and undisturbed species was performed to promote the discovery of potential, novel inhibitors of MEP synthase.

Examination of specimen morphology was used to determine taxonomy. Literary reviews were performed based on the taxonomy to assess whether prior research presented a medicinal (mainly, antimicrobial) value for the specimens identified.

2. Screen the library with recombinant *Y. pestis* MEP synthase.

Expression of recombinant MEP synthase in the laboratory strain of *E. coli* was necessary to yield adequate quantities of the purified protein to screen the molecular library and evaluate the inhibitory properties of the organic extracts. Due to its well-known potency as a MEP synthase inhibitor, FR900098 was used as a reference (positive control) for potent enzymatic inhibition. An extract was considered a significant hit if it demonstrated 75% or greater inhibition of enzyme activity.

3. Perform secondary screenings with bacterial growth inhibition assays on hit extracts.

Bacterial growth inhibition secondary screenings assessed the ability of hit extracts to inhibit the proliferation of *Y. pestis* cultures *in vitro*. Extracts that demonstrate an inhibitory effect on both the purified enzyme and the bacterial cells are preferred.

4. Determine the mechanism of inhibition for hit extracts.

Enzyme kinetic assays utilizing purified, recombinant MEP synthase were performed to measure the inhibition effect on enzymatic activity and to characterize the mechanism of inhibition with respect to DXP and NADPH. While competitive inhibitors of MEP synthase are valuable, allosteric inhibitors of the enzyme are preferred as their inhibitory activity is not suppressed by substrate accumulation.

5. Isolate and identify the active molecule.

A combination of ultra-centrifugation affinity chromatography and ultra-high performance liquid chromatography-mass spectrometry was used to purify the active inhibitor from the natural product extract. Tandem MS (MS/MS) was used to ensure definitive identification of the active metabolite. Extracted compound chromatogram (ECC) provided a clarified chromatographic reference of the retention times, accurate mass, and abundance for specific molecules from the total ion chromatogram (TIC) of the analyte. LCMS/MS spectra for specific molecules facilitated the identification of metabolites by manual comparative analysis with the reference MS/MS spectra from METLIN database [30].

6. Bulk purify, synthetically prepare, or commercially purchase the identified active compound.

Following the identification of the hit metabolite from the natural product extract, additional assays were performed to compare the inhibition by the raw extract with that of the pure standards for the identified lead compound. Since the active metabolite was commercially

available, bulk purification and/or synthesis was unnecessary. The commercially available compound was assessed for inhibitory activity in both enzyme-based and whole-cell based assays.

MATERIALS AND METHODS

Natural product extraction

The taxonomy for the collected specimens of botanical and fungal origin was determined subsequent to field surveys of wetland, meadow, and forest ecosystems. Each sample was measured to 1 g, frozen with liquid nitrogen, ground into fine powder with mortar and pestle, mixed with 15 mL ethyl acetate (Sigma-Aldrich, St. Louis, MO), and incubated for 30 min at room temperature. The mixture was then vacuum-filtered using Büchner Funnel filtration. Filtrate was subsequently collected and transferred to a round-bottom flask. The flask was placed on a Buchi Rotovaporator with the water bath temperature set to 44°C for rotary evaporation of the solvent. Samples were then resuspended in 1.0 mL ethyl acetate to allow the residue to be transferred into a 1.5 mL microcentrifuge tube. In order to produce a dry residue, aliquots were processed in a Savant SpeedVac centrifugal evaporator at 45°C (heat time: continuous, CCC; run time: 2.5 h). Each residue was weighed and stored at 4°C. Working solutions were prepared by resuspending dry extract residues in dimethylsulfoxide (Fisher Scientific, Waltham, MA) to a concentration of 10 mg/mL.

Purification of recombinant *Y. pestis* MEP synthase

The following procedure for the purification was implemented, as originally described by Haymond et al. [8]:

Seed cultures of bacteria were grown in 10 mL of Miller Luria-Bertani (LB) Broth (Fisher Scientific) supplemented with 100 µg/mL ampicillin (Research Products International Corporation, Mt. Prospect, IL) and 50 µg/mL chloramphenicol (Calbiochem, San Diego, CA). Two seed

cultures were prepared by inoculating the broth with a frozen glycerol stock of *E. coli* BL21 CodonPlus (DE3)-RIL+pYpIspC that was prepared as described in Hammond et al. [8]. The seed cultures were incubated in a New Brunswick Scientific Incubator Shaker I26 (250 rpm) at 37°C for 18 h. Next, each seed culture was added to a separate 1 liter LB Broth, subsequent to the broth being autoclaved and supplemented with 100 µg/mL ampicillin and 50 µg/ml chloramphenicol. The mixture was then returned to the incubator Shaker until the optical density at 600 nm (OD_{600}) reached a value of 1.8. Then, 0.5 mM isopropyl β-D-thiogalactopyranoside (IPTG) was added and the cultures were incubated for 18 h to produce recombinant histidine-tagged *Y. pestis* MEP synthase. The cells were harvested by centrifugation (4650 ×g) at 4°C for 20 min, weighed, and then stored at -80°C.

To purify recombinant MEP synthase, the frozen pellet was lysed with Lysis Buffer A (100 mM Tris-HCl pH 8 (Fisher Scientific), 0.032% w/v lysozyme (Sigma-Aldrich, Montana, USA) and Lysis Buffer B (0.020% w/v DNase, 0.1 M CaCl₂ (Sigma-Aldrich), 0.1 M MgCl₂ and 0.1 M NaCl (Fisher Scientific). The solution was centrifuged (48,000 ×g) for 20 min to yield a clarified supernatant, which was transferred to a TALON immobilized metal affinity column (Clontech Laboratories, Mountain View, CA) for protein purification. The column was then purged with 20 column volumes of equilibrium buffer containing 50 mM HEPES (BDH, Poole Dorset, UK) pH 7.5, 30 mM NaCl (Sigma-Aldrich), followed by 10 column volumes of wash buffer containing 50 mM HEPES pH 7.5, 300 mM NaCl, 10 mM imidazole (Sigma-Aldrich). An additional wash was performed by administering two cycles of 15 column volumes of wash buffer containing 100 mM HEPES pH 7.5, 600 mM NaCl, and 20 mM imidazole. Recombinant MEP synthase was eluted with 5 column volumes of elution buffer (150 mM imidazole pH 7.0, 300 mM NaCl). Buffer was exchanged with swap buffer solution containing 0.1 M Tris pH 7.5, 1 mM NaCl, and 5 mM DTT (Sigma-Aldrich) while the protein was concentrated by ultrafiltration. Gamma-globulins (Sigma-Aldrich) were used as protein concentration standards and the Advanced Protein Assay Reagent (Cytoskeleton, Inc., Denver, CO) was used to determine protein concentration. Coomassie

stained SDS-PAGE was used to visually assess the purity of the protein. The EZ run Protein Ladder (Fisher Scientific) was used as a reference to assess purity based on the target molecular weight of 46.7 kDa for the recombinant *Y. pestis* MEP synthase.

Bacterial growth inhibition assay

Y. pestis A1122 was obtained through the National Institute of Health (NIH) Biodefense and Emerging Infections Research Resources Repository, National Institute of Allergy and Infectious Disease (NIAID), as described by Hammond et al. [8]. Cultures of *Y. pestis* A1122 were grown overnight in 5 mL tryptic soy broth (TSB) supplemented with 0.1% w/v cysteine, using sterile 15 mL polypropylene tubes. The cultures were incubated at 25°C on a rotating incubator (250 rpm) for 24 h. The cell pellet was then harvested by centrifugation (2450 ×g) at 25°C. The cell pellet was washed twice by resuspending in 1 mL TSB, homogenizing by inversion and centrifuging for 15 min at 25°C. Following dilution with TSB, the OD₆₀₀ was assessed for an aliquot of the cell media, followed by the subsequent dilution with TSB until an OD₆₀₀ of 0.2 was achieved. Then, 170 µL TSB, 17 µL bacterial inoculum, and 8.5 µL natural product extract were added to each well of a 96-well plate. For dose-response assays with select inhibitors, *Y. pestis* cultures were instead dispensed into 10 × 1 cm foam-capped glass test tubes that contained 2 mL TSB, 200 µL inoculum, and 100 µL inhibitor at variable concentrations starting with initial 100 µM standards or 10 mg/mL natural extracts. The variable concentrations of each inhibitor were prepared using serial dilution with DMSO. Each dose-response assay was performed in duplicate. OD₆₀₀ of each bacterial culture was monitored for a 24 h period. Nonlinear regression was fitted to a standard dose-response plot using GraphPad Prism v4.00 for Windows and the equation for fractional velocity (F) to assess cell growth in response to inhibitor concentration, as described by Haymond et al. [8]:

$$F = \frac{1}{1 + \frac{[I]}{IC_{50}}}$$

Where $[I]$ = inhibitor concentration and IC_{50} is the concentration of inhibitor at half-maximal inhibition [8]. The IC_{50} for the validated inhibitor hit from the natural product extract was determined via a dose-response plot of cell growth (OD_{600}).

Enzyme kinetic assays

As described previously by Haymond et al. [8], assays were performed with purified, recombinant MEP synthase to measure enzyme activity by monitoring the enzyme-catalyzed oxidation of NADPH at 37°C at 340 nm with a UV-Vis spectrophotometer [8]. Each MEP synthase assay was performed in duplicate. The assay solution was composed of MilliQ H₂O, 100 mM Tris-HCl (Fisher Scientific) pH 7.8, 25 mM MgCl₂ (USB Corporation, Cleveland, OH), 0.89 μM MEP synthase, and 100 μM of the standard inhibitor. In the case of molecular library screening, 1.7% w/v natural product extract was administered in place of the 100 μM of standard inhibitor. After incubating the assay solution for 10 min at 37°C, 150 μM NADPH was added and incubated for an additional 5 min. In order to initiate the enzymatic reaction, 252 μM 1-deoxy-D-xylulose 5-phosphate (DXP; Echelon Biosciences, Salt Lake City, UT) was added immediately prior to spectrophotometrically monitoring the reaction progress. To determine the IC_{50} of the inhibitors, variable concentrations of the inhibitors were tested using standard assay conditions to assess and plot enzyme fractional activity as a function of inhibitor concentration. Nonlinear regression fitting a dose-response plot was accomplished using GraphPad Prism v4.00 for Windows. The aforementioned equation for fractional velocity was applied to determine the IC_{50} where F represents the catalytic activity [31]. Lineweaver-Burk plots were used to determine the modality of inhibition by monitoring MEP synthase activity at various inhibitor concentrations

under two separate test conditions: 1) with variable DXP and NADPH fixed at 150 μM (saturation) and 2) with variable NADPH and DXP fixed at 252 μM (K_M).

Affinity chromatography purification of the inhibitory compound from extract

To isolate the MEP synthase inhibitor from the e29 natural product extract, 1.5 mL samples were prepared containing 50 mM Tris-HCl, 25 mM MgCl_2 , 150 μM NADPH, 1.8 μM MEP synthase, and 3.3% w/v natural product extract. An additional 1.5 mL sample was prepared without e29 extract for comparative analysis. Each aliquot was preincubated at 37°C for 15 min. Each sample was then transferred into separate Amicon Ultra 30 kDa filter centrifugal concentrators (EMD Millipore, Darmstadt, Germany). A 500 μL aliquot of an aqueous wash buffer (50 mM Tris pH 7.8; 25 mM MgCl_2) was pre-equilibrated to 37°C and added to each concentrator and the samples were centrifuged in an Eppendorf 5810R at 3500 $\times g$ for 30 min at 25°C. The retentate was transferred from filter reservoir of the concentrator to a sterile 2 mL microcentrifuge tube, and an equal volume of pure MilliQ H_2O was added. Samples were incubated at 65°C for 25 min for protein denaturation, transferred to Amicon Ultra 10 kDa concentrator (EMD Millipore), and then centrifuged at 4000 $\times g$ for 60 min at 30°C. The filtrate was collected, snap-frozen, and stored at -80°C until LCMS analysis.

Liquid chromatography and mass spectrometry

Samples were removed from the -80°C freezer and diluted by 50% with LCMS Grade acetonitrile (Fisher Scientific), filtered using the Supelco (54145-U) Iso-disc, N-4-2 nylon, 4 mm x 0.2 μm filters (Sigma-Aldrich), and transferred to high-recovery amber vials (Agilent Technologies, Inc., Santa Clara, CA). Reverse-phase liquid chromatography was performed on the purified analyte using an Agilent 1290 Infinity Ultra High-Performance Liquid Chromatography system (UHPLC). The mobile phase was delivered by a binary pump at a flow rate of 0.4 mL/min. Solvent A was composed of LCMS Grade water + 0.1% v/v formic acid (Proteochem,

Loves Park, IL) and solvent B was composed of LCMS Grade acetonitrile + 0.1% v/v formic acid (Proteochem). The solvents were dispensed over a gradient: 0-1 min, 5% solvent B; 10 min, 30% B; 15 min, 70% B; 22 min, 90% B; 24-25 min, 100% B; 27 min, 2% B; 30 min, 5% B. The autosampler was set with an injection volume of 5 μ L. The flush port was set to clean injection needle for 30s intervals. A ZORBAX Rapid Resolution High Throughput (RRHT), 2.1 x 50 mm, 1.8 μ m C18 column (Agilent Technologies, Inc.) was used. The column was maintained at an isothermal temperature of 38°C. Mass spectrometric analysis was performed by an Agilent 6530 Quadrupole Time of Flight (QTOF) LCMS with an electrospray ionization (ESI) source set for detection mass range from mass-to-charge ratio (m/z) 100 to 1000. A dedicated isocratic pump continuously infused reference standards of purine (Agilent Technologies, Inc.) and hexakis-H, 1H, 3H-tetrafluoropropoxy-phosphazine, or HP-921 (Agilent Technologies, Inc.) at a flow rate of 0.5 mL/min to achieve accurate mass correction. The nebulizer pressure was set at 35 psig with a surrounding sheath gas temperature of 350°C and a gas flow rate of 11 L/min. Drying gas temperature was set at 300°C with a flow rate of 10L/min. Default settings were used to set voltage gradient for nozzle at 1000 V, skimmer at 65 V, capillary (VCap) at 3500 V, and fragmentor at 175 V. Each cycle of acquisition was performed at a constant collision energy that varied between 0, 10, 20, and 40 volts for subsequent tandem MS analysis. In the time-of-flight tube, the mass is generally determined on the basis of travel time given that ions with the same charge are expected to have the same kinetic energy (KE) [32, 33]. The KE is the product of the charge (z) of the ion and the voltage (V) applied by the pulser to accelerate ions to reach the detector, as shown in the following equation:

$$KE = zV = \frac{1}{2} m \left(\frac{L}{t} \right)^2$$

Thus,

$$\frac{m}{z} = \frac{2Vt^2}{L^2}$$

Here, m refers to the molecular mass; L , the length of the flight tube; and t , the time it takes the molecule to travel through the flight tube and reach the ion detector [32, 33]. Agilent MassHunter Acquisition SW Version, 6200 series TOF/6500 series Q-TOF B.05.01 (B5125.1) was used to record LCMS data. Agilent MassHunter Qualitative Analysis B.06.00 was used to analyze data and to generate the total ion chromatogram (TIC), extracted compound chromatogram (ECC), and mass spectra for analyte compounds. To enhance differential analysis, adjustments were applied to the purified analyte (containing the inhibitory extract) data wherein Auto MS/MS and MS compound analysis method was configured to exclude the m/z for the parent ions that were previously detected at a high abundance ($\geq 1.0 \times 10^7$ counts) in the spectrum for the control sample (containing the only preparatory solution for the purification process without the inhibitory extract). The excluded ions were defined in the Chromatogram and Find Compound methods. As a result, most of the characteristic features of the preparatory solution were eliminated from the chromatogram of the purified analyte. Consequently, the resolution and retention times for unique features that were only associated to the purified analyte became well-defined. This allowed a clear differentiation between the characteristic peaks in the TIC of the purified analyte from those detected in uninhibited control. In general, MS acquisition was performed with a two replicate injections to allow column conditioning and examine reproducibility. Tandem mass spectra were processed using the Find Compound by MSMS function to envelope product ions and related features (adducts, isotopes, and fragment ions that elute at the same retention time). Mass spectra of compounds detected in the samples were processed using the Find Compound by Options function set to consider factors including sodium (Na^+) and hydrogen (H^+) adducts and neutral loss of water (H_2O) while utilizing the METLIN Metabolite Personal Compound Database add-in for Agilent MassHunter Qualitative Analysis B.06.00. The initial step in the identification of metabolites relied on the METLIN Metabolite PCD match-scoring criteria filters that was used to evaluate the m/z for potential adducts, potential neutral loss, accurate mass, and isotope effect to calculate and propose

chemical formula matches for precursor ions [34]. Follow-on manual comparative analysis of raw tandem MS data was performed with online MS/MS spectra library references as described stepwise in Appendix D.

Hydrolysis of glycoside

To hydrolyze the glycosides present in the natural product extracts and release their aglycone, thereby further validating the identification of the active inhibitor present in the extract, 300 μ L aliquots of the extract were incubated with 1.2 mM HCl (Fisher Scientific) at 70°C in a water bath (Fisher Scientific Isotemp 215). Incubation was performed at 1 h, 3 h, and 24 h intervals. Prior to LCMS analysis, all samples were centrifuged using Eppendorf 5415D for 3 min at 16.9×10^3 xg. All samples were subsequently analyzed using Agilent 6530 QTOF LCMS coupled with 1290 Infinity UHPLC.

RESULTS AND DISCUSSION

Molecular screening of a natural product library

Investment in pharmacognosic research which involves bioprospecting can lead to the discovery of novel antimicrobial treatments and elucidate novel drug target sites. Plant and microbial organisms contain metabolic pathways that are specialized to biosynthesize thousands of secondary metabolites with high specificity for target enzymes in critical biochemical pathways of other organisms (e.g. pathogenic microbes). Thus, bioprospecting was once the primary source for novel drug discovery [25]. Although the majority of medications available on the market can be traced back to natural products and their derivatives, bioprospecting has been replaced by alternative drug development approaches [26]. Other approaches such as combinatorial chemistry are known to produce a high volume of drug candidates for high-throughput screening, while often resulting in a low yield of viable candidates [26]. In addition, other drug development approaches often rely on derived analogs of broadly used drug treatments [26]. The main drawback to the complete reliance on these analogs is that pathogens who inherit mechanisms of resistance for a specific antibiotic can, in turn, adapt to their derivatives due to the similarities in structure and mode of activity [14].

Historically, the use of bioprospecting has provided a starting point for the development of drug treatments and molecular libraries with a broad range of bioactive compounds [25, 28]. One major drawback that led to a decline in pharmacognosic research is the impediment associated with isolating and identifying active components from the complex matrices of extract with hits. Now, with modern UHPLC-QTOF coupled with advancements in chromatography,

molecular databases and data mining, low-abundance metabolites can be definitively isolated and identified from a complex matrix of nonspecific metabolites.

In this pharmacognosic research, recombinant *Y. pestis* MEP synthase was used to detect and isolate potential antimicrobial candidates through molecular library screening. Haymond et al. [8] established that the assay involving the *Y. pestis* MEP synthase is well suited for molecular library screening. In addition, MEP synthase is the first committed step in the MEP pathway and is a well-validated target for the development of novel antibiotics.

The assays used to complete the molecular screening of the natural product library were performed in duplicate using recombinant *Y. pestis* MEP synthase. Residual enzymatic activity for MEP synthase was measured relative to the uninhibited sample, which represented no inhibition. FR900098 is a well-known potent inhibitor for MEP synthase and was included in the molecular screening to serve as a reference for a potent hit.

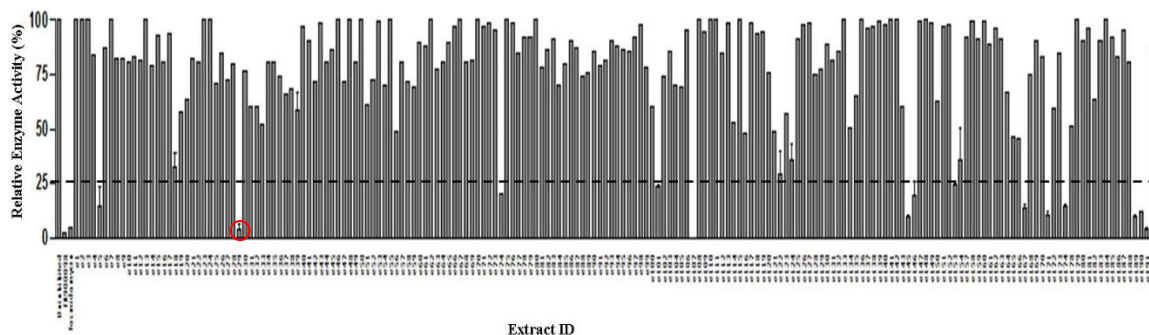


Figure 3: Molecular screening of the natural product extracts.

Figure 3 displays the results of the molecular screening for the complete in-house library of 192 unique extracts obtained from diverse biological sources. In the analysis, the threshold for a good hit was set at 25% residual activity (represented by cut-off line in Figure 3); thus, a 75%

inhibition. Multiple natural product extracts (including e29, e74, e107, e145, e146, e154, e167, e171, e174, e189, e190, and e191) demonstrated $\geq 80\%$ inhibition of the MEP synthase activity. As shown in Figure 3, the results of the molecular library screening revealed that e29 (derived from *Rumex crispus*) demonstrated a 96% inhibition, comparable to the inhibitory effect of fosmidomycin (95% inhibition) and FR900098 (98% inhibition). Therefore, e29 (highlighted in red) was selected for further characterization and identification of the active inhibitor.

Bacterial growth inhibition for *Y. pestis* with extract 29

Due to its potent activity against the recombinant MEP synthase, e29 was selected for follow-on evaluation of whole-cell inhibition using liquid cultures of *Y. pestis* A1122. Growth inhibition assays were performed to evaluate the susceptibility of *Y. pestis* A1122 cultures to the active inhibitor from e29 in a dose-dependent manner. Given that a natural product extract was used for this study, the estimated concentration of the e29 inhibitor present in the extract was initially unknown. However, dose-dependent growth inhibition was sought to justify the additional investment necessary to isolate and identify the active metabolite in e29.

The standard dose-response plots were generated for liquid cultures of *Y. pestis* by spectrometrically monitoring OD₆₀₀ vs. time. Growth inhibition assays were performed in duplicate and measurements were taken over a 24-hour period. The percent bacterial growth at each concentration of e29 was determined, relative to the uninhibited control which was not administered the inhibitory extract.

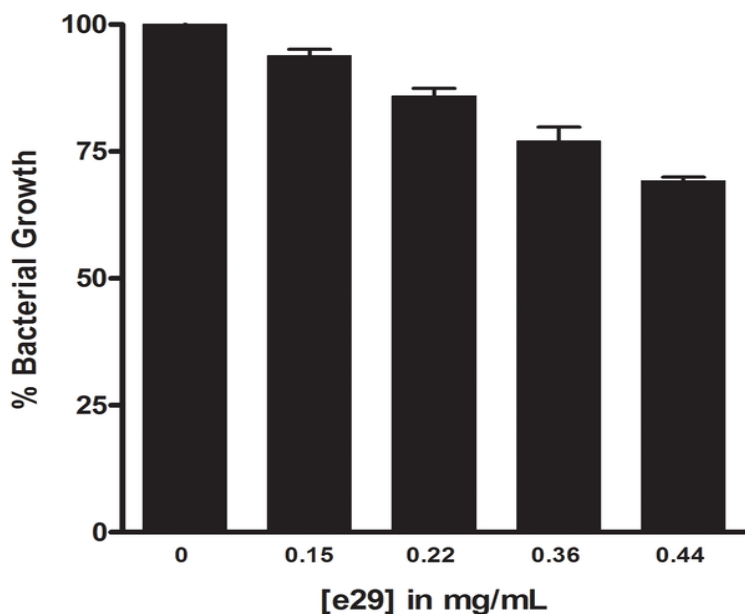


Figure 4. Bacterial growth inhibition assays for *Y. pestis* with extract 29.

As shown in Figure 4, the *Y. pestis* growth rates declined by 30% in the presence of 0.44 mg/mL of e29, compared to the control culture. Overall, the plot illustrates that the active compound in e29 inhibited *Y. pestis* proliferation in a dose-dependent manner, relative to the uninhibited control. These findings suggest that the e29 inhibitor hit should present a dose-dependent bacteriostatic effect for growth cultures of *Y. pestis* following isolation and identification of the lead inhibitor.

Identification of a novel inhibitor in extract 29

As previously discussed, one of the known challenges in screening a natural product library is the cost and difficulty associated with the separation and identification of active compound(s) from a raw extract [25]. In this research, affinity chromatography was applied to purify the active inhibitor from nonbinding compounds in the raw e29 extract. This affinity chromatography method was based on the affinity between MEP synthase and the active

component in the e29 extract. It was anticipated that this approach would concentrate the active compound(s) due to their biospecificity and affinity for the binding sites on MEP synthase, resulting in an enhanced detection of the compound while reducing background from the extract matrix during the mass spectrometric assay.

To perform the affinity chromatography procedure, the extract was incubated with MEP synthase and NADPH to allow binding of the active inhibitor. An additional sample was prepared without the extract to serve as a blank (negative control) for comparative LCMS analysis. Ultracentrifugation was performed using a filtered centrifugal concentrator to allow the unbound components to be eliminated with the filtrate. The retentate (containing the enzyme in complex with an inhibitor) was collected and denatured to release the inhibitor from its binding site.

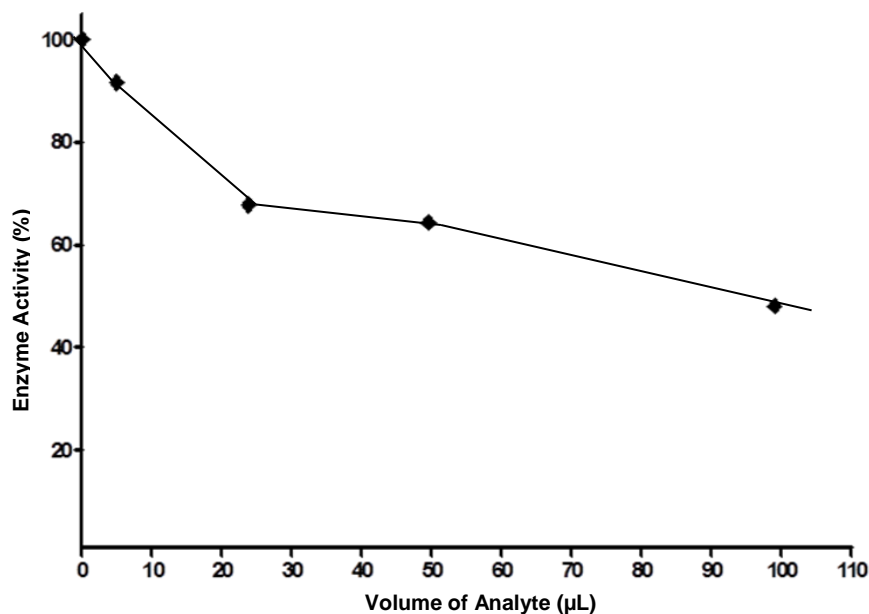


Figure 5. Enzyme kinetic assays with purified analyte using *Y. pestis* MEP synthase.

Following the implementation of the affinity chromatography method, qualitative enzyme assays were performed to verify that the inhibitor was retained in the affinity purified analyte.

Purified, recombinant *Y. pestis* MEP synthase was used to perform assays with the purified analyte at incremental volumes of 0, 25, 50, and 99 microliters of analyte. In order to maintain standard assay conditions, the volume of MilliQ H₂O used in the assay solution was adjusted to accommodate for the increasing volumes of the purified analyte that were tested to detect a dose response. As shown in Figure 5, the purified analyte demonstrated dose-dependent inhibition of MEP synthase. Moreover, the purified analyte presented a 52% inhibition of MEP synthase activity when assayed at a volume of 99 μ L. This finding suggested that the purified analyte retained the active inhibitor in a diluted solution. If the active inhibitor had not been retained during the purification process, the enzyme would not have demonstrated a dose response to the purified analyte. This qualitative assessment confirmed that the affinity purified analyte retained its dose-dependent inhibition of MEP synthase activity, which provided sufficient evidence to proceed with a spectrometric analysis of the analyte.

In order to identify the MEP synthase inhibitor, the affinity purified analyte was processed using liquid chromatography coupled with tandem mass spectrometry (MS/MS). Tandem MS (specifically, QTOF) generates unequivocal data to determine the fragmentation patterns, molecular features, and chemical formula of metabolites. For this experiment, collision energies of 10, 20, and 40 volts were selected so as to be consistent with references from the online METLIN database [30].

The parameters for the MS/MS method were optimized by tuning the QTOF instrument to identify individual metabolites as they elute from the HPLC column, based on set specifications for detection of molecular features (including adducts, neutral losses, isotopes, and associated fragment ions) [35]. In order to extend beyond the automated algorithm used by the Masshunter software for the identification of metabolites, a manual comparison of MS and MS/MS reference spectra was performed to ensure a robust analysis. In addition to using commercial standards, the analysis included an assessment using the reference spectra that were available through the

online METLIN database, which were also generated on an Agilent ESI-QTOF instrument [30, 34].

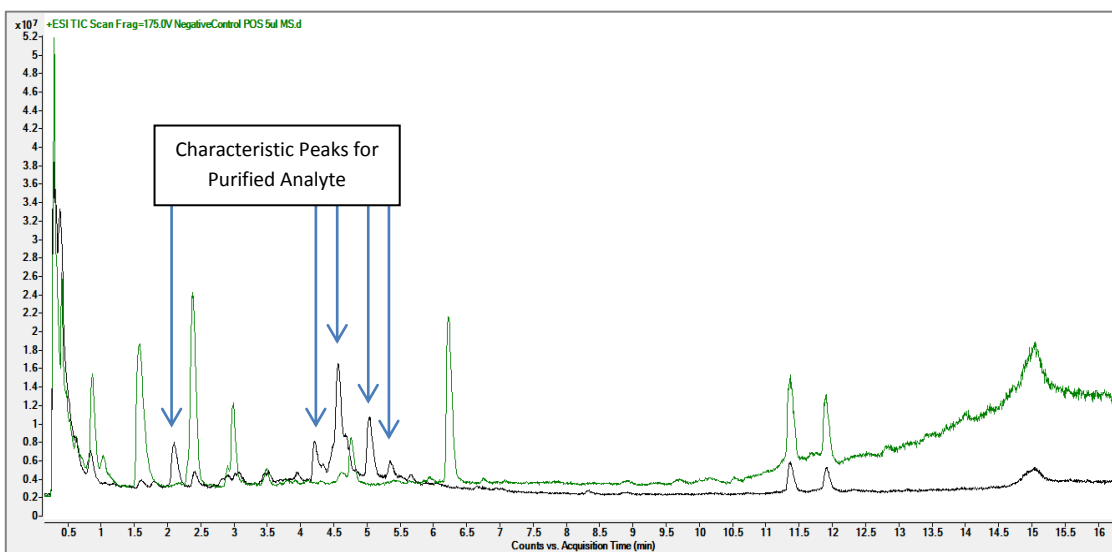


Figure 6. Chromatograms of the uninhibited control (green) and affinity purified analyte (black) for comparative analysis.

Figure 6 provides an overlay of the total ion chromatograms (TICs) for the uninhibited control (green) and the purified analyte (black). The chromatogram for the control (containing only the preparatory solution used in the purification process without the inhibitory extract) presented multiple peaks that were clearly characteristic of the purification solution prepared in absence of the e29 extract. The masses of ions detected in the control with abundances exceeding the preset threshold ($\geq 1.0 \times 10^7$ counts) were excluded from the TIC of the purified analyte. This approach allowed the signal for unique features within the analyte to be more resolved while suppressing background from the preparatory solution. The chromatograms and spectra that were generated during the LCMS profiling of the purified analyte were evaluated for unique chromatographic peaks and precursor ions, which were then determined to be the defining features of the purified analyte.

In Figure 6, a comparative analysis of the TIC overlay for the two groups revealed that there were five main peaks of interest (represented by arrows occurring at the retention times (RT) of 2.1, 4.3, 4.5, 5.0, and 5.4 minutes), which represented defining features that were only present in the TIC for the purified analyte. Meanwhile, the initial peak (RT: 0.5 min) that occurred during the aqueous mobile phase contained numerous low abundance, polar ions that eluted simultaneously. This resulted in an intense yet poorly resolved peak, for which the abundance of each individual ion detected in the control sample did not meet the criteria for exclusion during the profiling of the purified analyte. Therefore, many of these were common ions that remained in the TIC for the purified analyte.

To profile the low abundance and poorly ionized ions empirically, the full spectra were exported to Excel for empirical analysis. Given the dynamic range of ions detected, it was necessary to utilize empirical filtering and ranking procedures in order to prioritize compounds of interest. All common ions were determined and eliminated based on the agreement between m/z and retention time for ions detected in both the purified analyte and the control. The assumption was that given a particular set of constant conditions (e.g., column composition and temperature, mobile phase, flow gradient, flow rate, and sample matrix), the retention time and m/z for specific compounds would be reproducible. This assumption provided a preliminary approach to differentiate and characterize the broad range of compounds detected in the spectra. Isobaric ions of similar masses were grouped for re-assessment if they were within an m/z interval of ± 0.0010 and presented a variation in retention time that exceeded 1.0 min. The remaining masses were ranked by abundance.

For the enzyme target-affinity purification method, it was anticipated that the majority of the metabolites with weak or no interaction with the target would be filtered out during the washing steps. In turn, this was expected to enhance the detection of components based on their affinity for MEP synthase, while significantly reducing noise from nonspecific metabolites present

in the matrix of the inhibitory extract. The unique masses determined in the purified analyte that exhibited an abundance exceeding the set threshold (9.0×10^4 counts) were prioritized as the main compounds of interest. This prioritization narrowed down the list of compounds from 6.0×10^3 hits to 1.0×10^2 hits.

Evaluation of retention time, mass spectra, and isotope effect provided a guideline to determine which compounds had similar chemical formulas and/or identities. This approach led to the creation of ten categories which grouped compounds that were expected to be identical, isomers, or similar in chemical structure. Further comparative analysis of MS/MS spectra between the compounds within each category reduced the list to eight potential compounds.

By evaluating the m/z , accurate mass, and isotope distribution, it was possible to predict the chemical formula of the selected ions with a 98-99% confidence at a mass error ≤ 5 ppm. Meanwhile, the differential analysis of the tandem MS spectra provided a means to accurately assess which compounds were similar or uniquely different. Moreover, the use of tandem MS provided further confidence and evidence to determine the identity of the metabolites of interest from the vast number of reference library hits with a matching m/z , accurate mass, or chemical formula.

Table 1. Potential active compounds identified using tandem MS analysis.

Compound ID	Chemical Formula	Exact Mass (Da)	Mass-to-Charge Ratio (m/z)	Chemical Ionization	Retention Time (min)
quercetin	C ¹⁵ H ¹⁰ O ⁷	302.0427	303.0499±0.0005	[M+H ⁺]	4.570, 5.022, 5.056, 6.920
quercetin 3-β-D-glucoside	C ²¹ H ²⁰ O ¹²	464.0955	465.1022±0.0005	[M+H ⁺]	4.571
quercetin 3-galactoside	C ²¹ H ²⁰ O ¹²	464.0955	465.1022±0.0005	[M+H ⁺]	4.571
quercitrin	C ²¹ H ²⁰ O ¹¹	448.1006	449.1078±0.0006	[M+H ⁺]	5.056
±catechin	C ¹⁵ H ¹⁴ O ⁶	290.0790	291.0863±0.0002	[M+H ⁺]	2.145
epicatechin	C ¹⁵ H ¹⁴ O ⁶	290.0790	291.0873±0.0006	[M+H ⁺]	2.091
unconfirmed compound 7	C ²¹ H ¹⁸ O ¹³	478.0747	479.0821±0.0004	[M+H ⁺]	4.678
unconfirmed compound 8	C ²⁰ H ¹⁸ O ¹¹	434.0849	435.0921±0.0005	[M+H ⁺]	5.056

The putative identity, exact mass, mass-to-charge ratio (m/z), retention time, and ionization state for the eight potential compounds of interest are detailed in Table 1. In general, [M+H⁺] reflects the parent ions that are protonated with the hydrogen adduct. Based on the m/z, accurate mass, and isotopic effect, the chemical formulas that were defined for the confirmed and unconfirmed compounds presented a 98-99% confidence with a mass error ≤5 ppm. Meanwhile, the corresponding MS/MS reference from the online METLIN database was unavailable for the unconfirmed compounds [30]. Differential analysis was performed against the MS/MS spectra of similar compounds (i.e., those compounds with the same chemical formula or suspected to be within the same chemical family) in the online METLIN database [30]. Identification was based on the matching of the major fragment ions while tolerating mild variations in their intensities. In

the case of the unconfirmed compounds, their MS/MS spectra revealed that each precursor ion produced a major fragment ion with the same m/z as the quercetin (m/z 303.0499±0.0005). In addition, the m/z, accurate masses, and proposed chemical formulas for the unconfirmed compounds were well-matched to the references for other glycosides of quercetin available in the online METLIN database [30]. Therefore, it was predicted that these unconfirmed compounds were glycosides of quercetin as well.

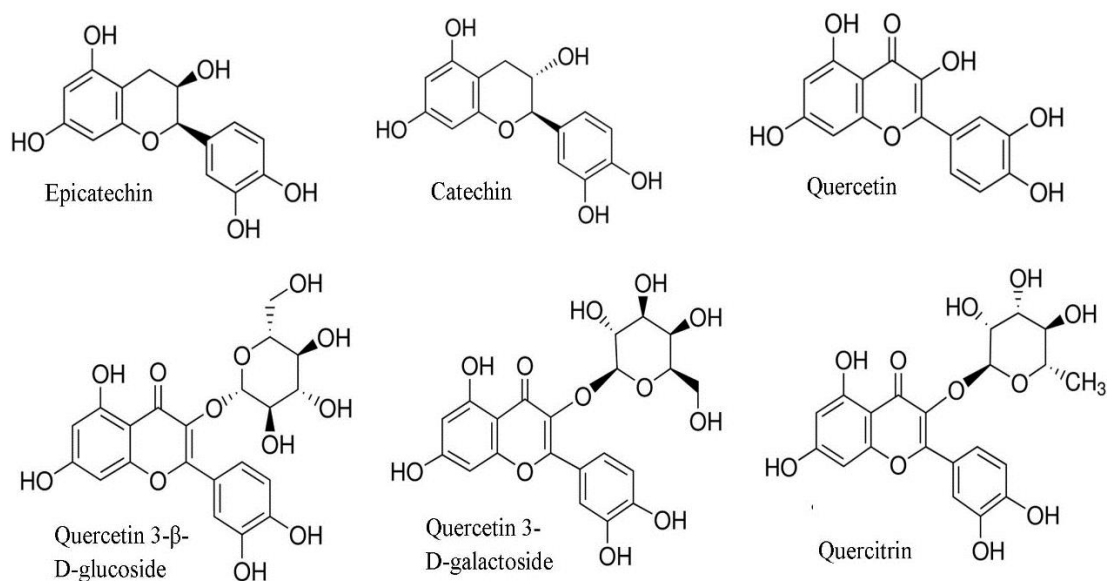


Figure 7. Potential active compounds detected in the purified analyte.

Following the processing of the LCMS data, putative identities of quercetin, quercetin 3-β-D-glucoside, quercetin 3-galactoside, quercitrin, ±catechin, and epicatechin were proposed for the primary metabolites detected in the purified analyte, as shown in Figure 7. The results of the difference spectrum comparison between the tandem mass spectrometry (MS/MS) and the database references for the proposed identities of these potential active compounds are provided

in Appendix B. Tandem MS analysis was critical for the identification of the potential active metabolites detected in the purified analyte, given that this type of analysis permits precise differentiation between molecules characterized with the same mass and chemical formula.

Validation of the active inhibitor present in extract 29

The profiling of metabolites in the natural product extract relied on the detection and quantification of unique precursor ions and chromatographic peaks that were considered as defining features of the analyte. Differential analysis between the profiles of the analyte and uninhibited control provided insight about which metabolites were unique to the extract. Based on the outcome of the identification process, six primary compounds (i.e., quercetin, quercetin 3- β -D-glucoside, quercetin 3-galactoside, quercitrin, \pm catechin, and epicatechin) were selected for validation.

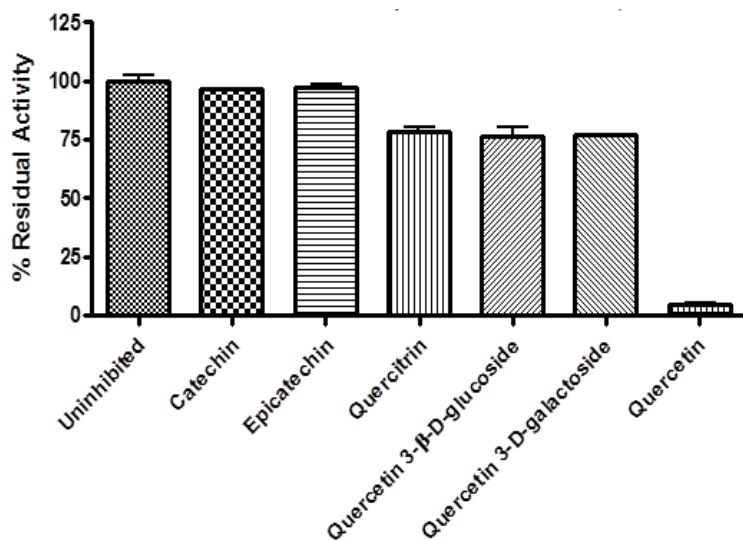


Figure 8. Comparisons of the inhibitory quality for potential active compounds present in the purified analyte.

Following prioritization, commercial standards of quercetin, quercetin 3- β -D-glucoside, quercetin 3-galactoside, quercitrin, \pm catechin, and epicatechin were purchased and assayed. A methodology similar to the rational library screening was used to prepare each standard at a concentration of 100 μ M, as described by Hammond et al. [8]. Assays were performed in duplicate with NADPH, DXP, and *Y. pestis* MEP synthase. As showed in Figure 8, the comparison of the prospective compounds revealed that quercetin (100 μ M) presented the most potent inhibition of MEP synthase. The enzyme kinetic assay with quercetin resulted in a 4.9% inhibition of the MEP synthase catalytic activity. In addition, the glycoside moieties of quercetin presented minor inhibitory effects on the MEP synthase activity. The negligible inhibition demonstrated by the glycoside moieties (quercetin 3- β -D-glucoside, quercetin 3-galactoside, and quercitrin) resulted in 78%, 76%, and 77% residual activity for MEP synthase, respectively. Based on the data (Figure 8), \pm catechin and epicatechin clearly did not present a substantial inhibition of MEP synthase, with respect to the uninhibited enzyme.

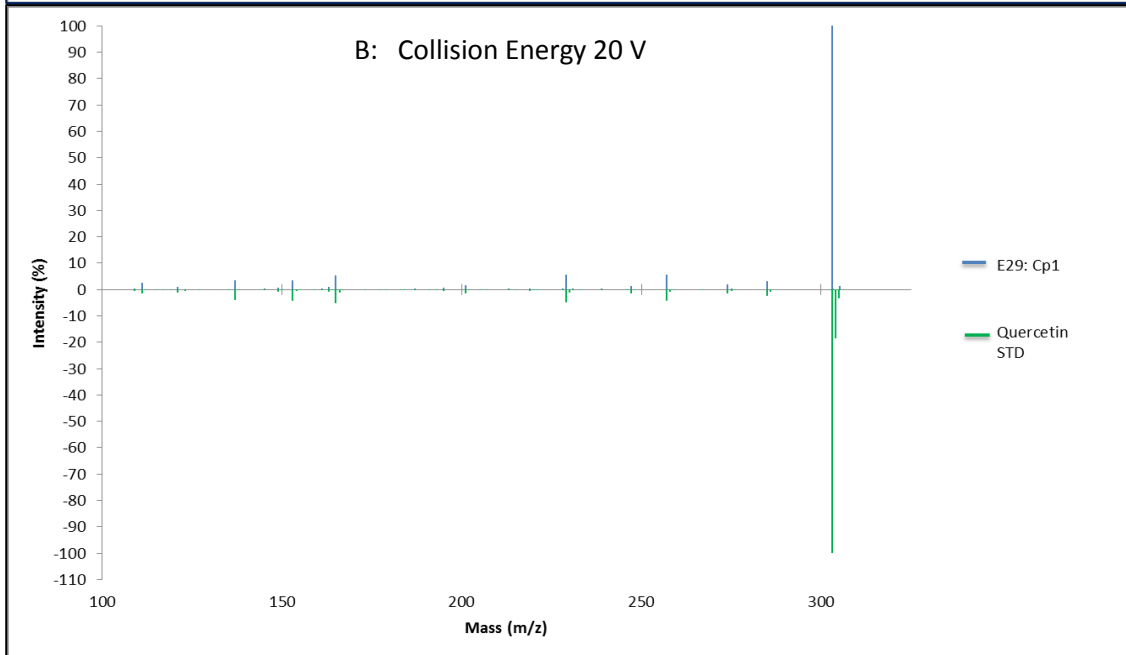
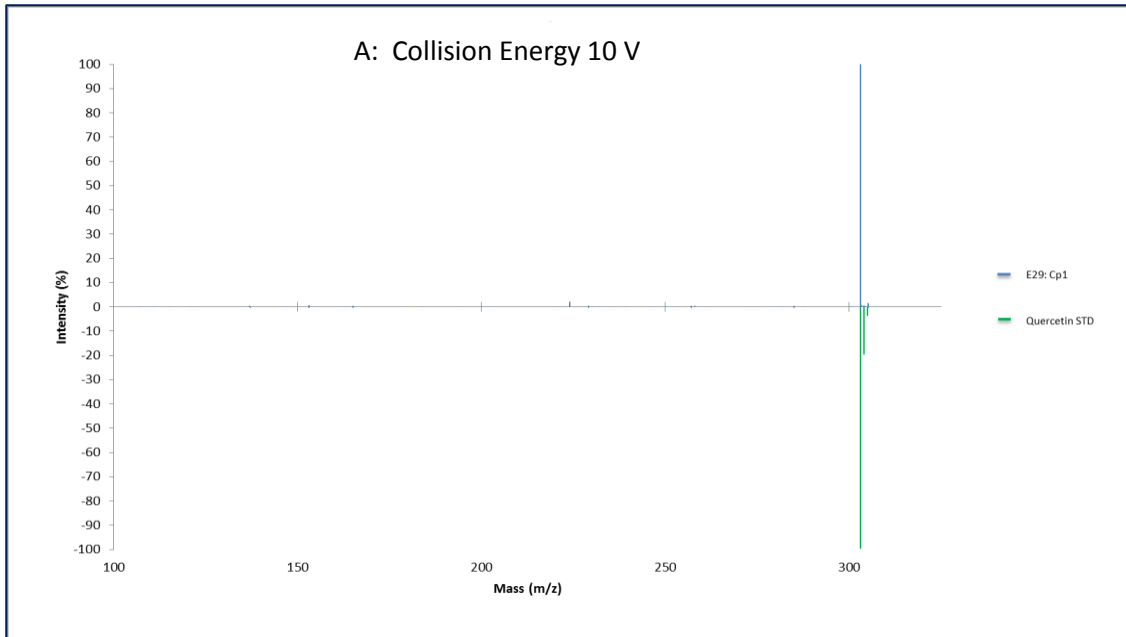
The quercetin and the aforementioned three glycosides are members of the flavonol class of flavonoids. Flavonol aglycones (such as quercetin) are secondary metabolites that are stored in glycosylated form until their metabolic activity is required [25]. Consequently, flavonol aglycones are typically detected in tandem with their glycone conjugates during mass spectrometric analysis [25]. The results of these assays suggest that the glycosylated moieties of quercetin likely introduced constraints that obstructed access to the allosteric binding site. The plot data presented in Figure 8 suggested that the presence of glycone limited the inhibitory quality of the quercetin conjugate.

In addition, the \pm catechin and epicatechin compounds that were assayed are members of the flavanol subclass of the flavonoid family [25]. In the case of the flavanols, the absence of the carbonyl on the central pyran ring may have rendered \pm catechin and epicatechin inactive even upon association with MEP synthase. Therefore, it was anticipated that the presence of a ketone

on the central pyran ring of the flavonol (such as quercetin) is necessary for the inhibitor to bind appropriately and elicit the conformational change that restricts the completion of the MEP synthase-mediated conversion of DXP to MEP.

Validation of the putative identity for the active inhibitor by MS/MS comparative analysis

Based on the complete analysis of potential active compounds, quercetin was designated as the principal candidate that exhibited the most potent inhibitory effect at a concentration of 100 μM by comparison. Furthermore, quercetin (302.0427 Da) met the guidelines provided by Lipinski and Glaxo Smith Kline (GSK) on mass criteria for compounds that can qualify as drug candidates (also referred to as drug-like space) [36]. The Lipinski drug-like space mass criteria permits an upper limit of 500 Da and the GSK permits up to 400 Da, while both stipulate a lower mass limit of 250 Da [36]. Compounds that are outside of drug-like space mass criteria tend to fail in drug development due to issues related to absorption, distribution, metabolism, excretion, and toxicity (ADMET) factors [36]. Given that the lead inhibitor candidate met the drug-like space mass criteria and outperformed the other potential active compounds during assays with MEP synthase, it was determined to be the best candidate for further validation.



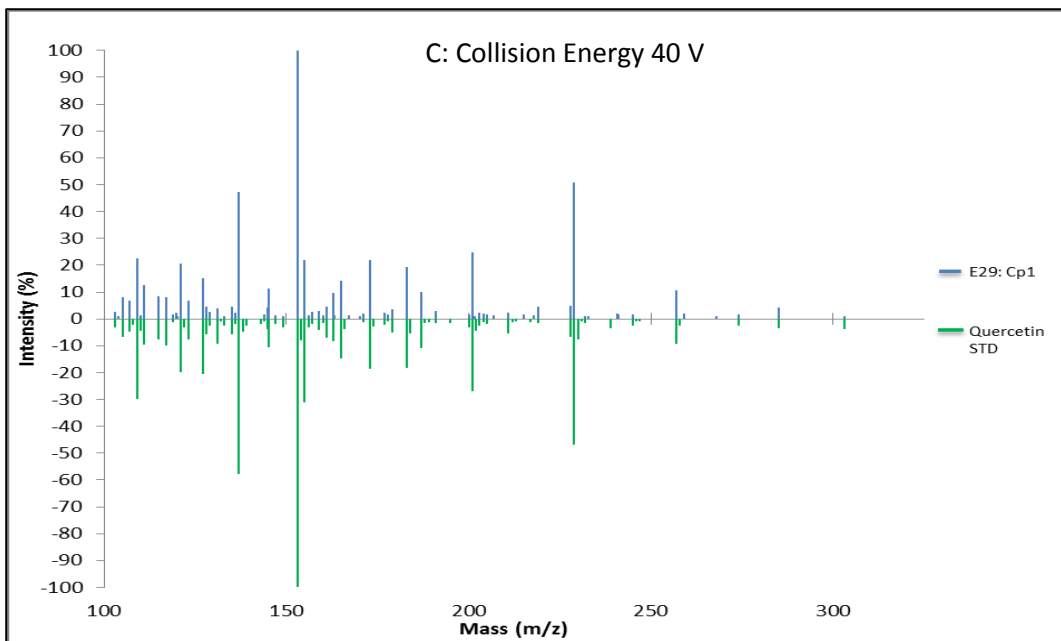


Figure 9. MS/MS comparative analyses for quercetin in extract 29 against quercetin commercial-grade standard at collision energies 10 V, 20 V, and 40 V.

A difference spectrum analysis (shown in Figure 9A-C) was performed to compare the tandem MS spectra for the quercetin identified in the purified analyte against a commercial-grade quercetin standard, under the same MS acquisition parameters. Based on the difference spectrum analysis, the prominent fragment ions of the quercetin detected in the purified analyte presented a clear alignment with the major fragment ions detected for the commercial-grade quercetin. The main variation occurred in the tandem MS spectra captured at 20 and 10 volts, wherein the isotopic peaks for the quercetin precursor ion (m/z 303.05) were only presented in the spectra for the commercial-grade quercetin at m/z 304.05 (M+2) and 305.05 (M+3), respectively. Other minor variations (e.g., difference in the abundance of fragment ions and appearance of minor unmatched ions) in the difference spectrum comparison were attributed to the variability in the ionization of the samples that likely resulted from dissimilarities in the sample

matrices. The overall agreement between the peaks for the precursor ion and the majority of fragment ions in the tandem MS spectra (Figure 9A-C) provided substantial evidence that quercetin was the actual identity of the lead allosteric inhibitor detected in e29.

Hydrolysis of potential quercetin glycosides in extract 29

In living systems, secondary metabolites such as the flavonol quercetin and other flavonoids are typically stored as sugars (glycosides) in their inactive form (through the catalytic activity of glycosyltransferase), until they are needed [37]. At which point, enzymatic hydrolysis by glycosidase activates aglycones by detaching the glycone conjugates of the glycoside [37, 38]. In other organisms, glycosidase in saliva (lysozyme), the digestive tract, and bacteria hydrolyze glycosides of flavonoids upon consumption [37, 39, 40]. In a laboratory setting, acid hydrolysis by sulfuric acid or hydrochloric acid is commonly applied to glycosides in order to liberate flavonoid aglycones for characterization and quantification [41, 42].

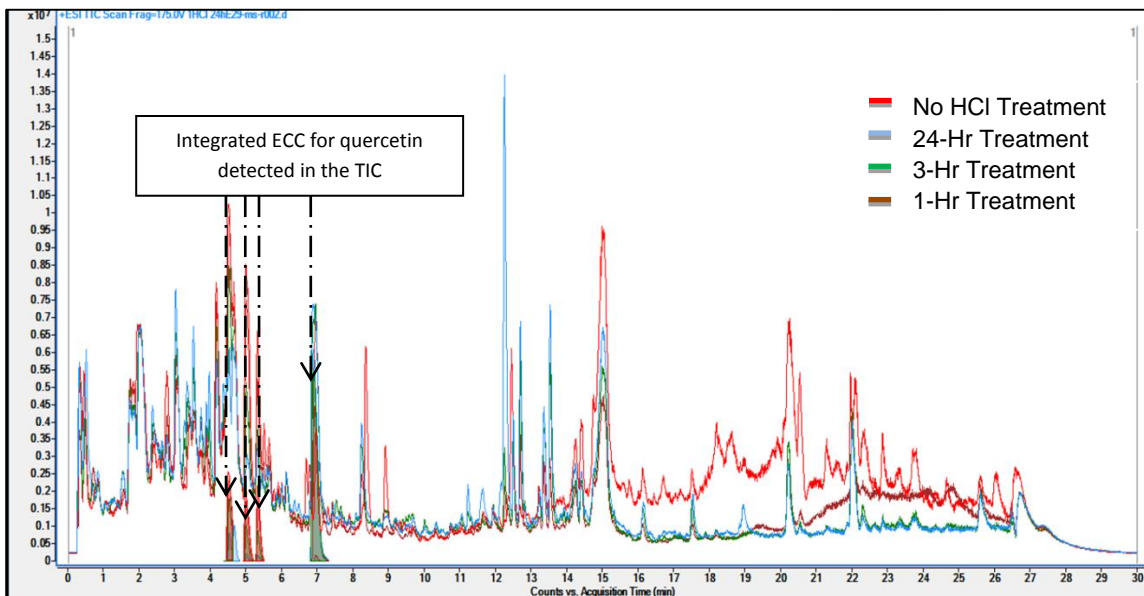


Figure 10. Extracted compound chromatogram of quercetin integrated with total ion chromatogram for each of the HCl-treated and untreated extract 29 analytes.

As part of the validation process, LC-QTOFMS analysis was performed on aliquots of the raw extract that had undergone acid hydrolysis with hydrochloric acid (HCl) for incremental periods of time. The total ion chromatogram (TIC) showed in Figure 10, which was generated from a full scan of the untreated raw extract, shows an overlay of the TIC for each sample that had been treated with HCl. The extracted compound chromatogram (ECC) for the quercetin precursor ions detected in each sample was represented by the shaded peaks, which were integrated with the overlay of their respective TIC. The ECC confirmed that there were multiple positions (representing the different retention times) where the quercetin ions (m/z 303.0499 \pm 0.0005) were detected in the analyte from the raw and HCl-treated extracts. This outcome was consistent with the findings for quercetin detailed in Table 1 (which summarized the differential analysis between the uninhibited control and the purified analytes). It was predicted that the quercetin ions that eluted early-on in the chromatogram were likely associated to highly polar, glycone conjugates. In order to clearly compare the differences in the quercetin detected in each sample, it was necessary to examine the deconvoluted ECC for the untreated and HCl-treated samples, as shown in Figure 11.

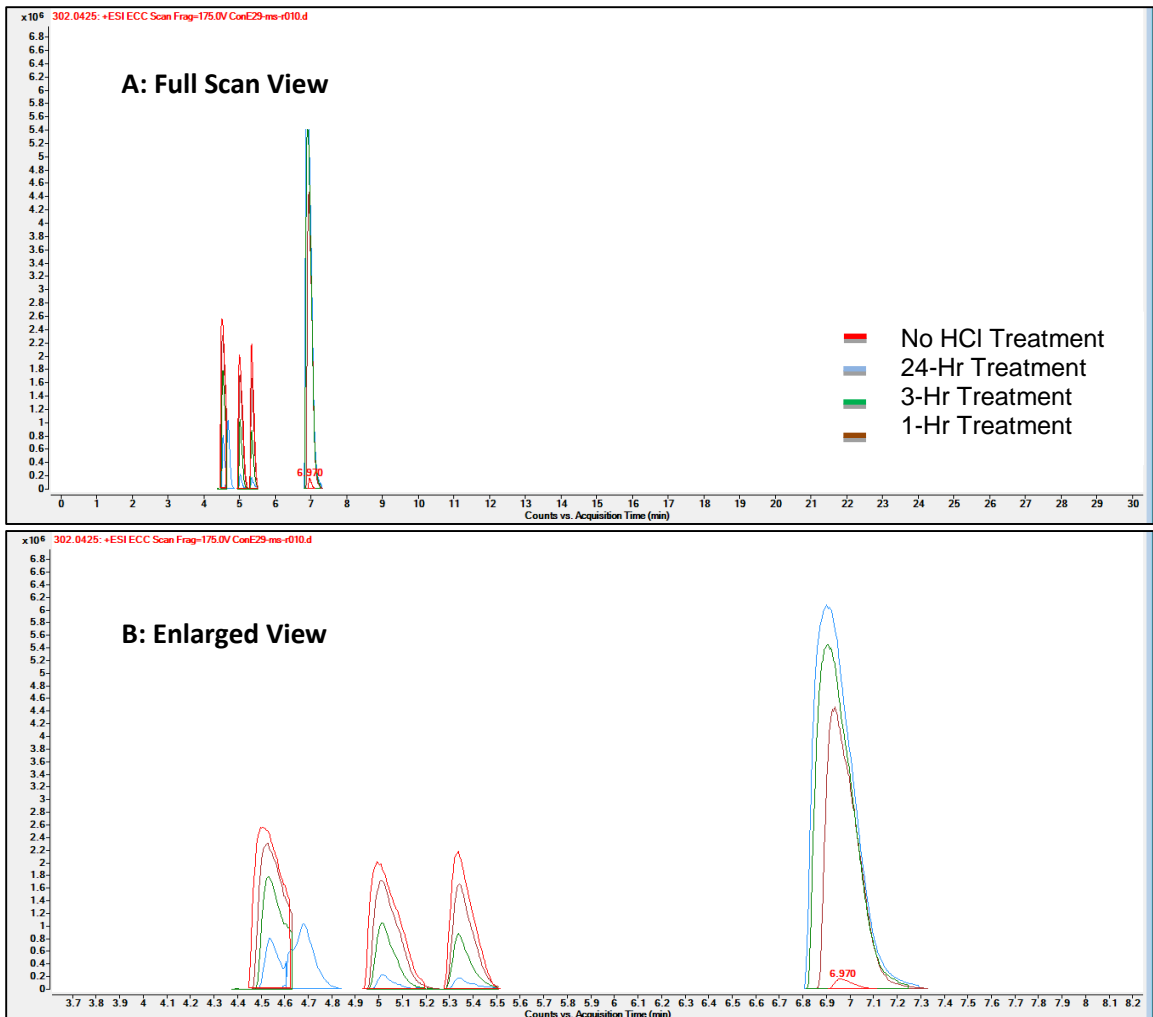


Figure 11. Extracted compound chromatogram of quercetin in the HCL-treated and untreated e29 analytes.

Figure 11 provides a clear comparison of the change in the appearance of quercetin ions following treatment of the raw extract with acid hydrolysis. For the experiment, aliquots of e29 were incubated at a constant concentration of hydrochloric acid (HCl) for incremental time periods (1h, 3h, and 24h treatment), in order to assess whether there was a change in the abundance of quercetin ions at the different retention times where these specific ions were detected in the analyte. For each sample, each precursor ion detected for quercetin was validated using tandem

MS analysis. The intent was to confirm that the precursor ions did not deviate from the expected fragmentation fingerprint defined for quercetin in both the standard and purified analytes (see Figure 9). In Figure 11, the ECC for the quercetin ions detected in each sample presented a prominent signal for quercetin at 6.92 min, following incubation of the raw extract with HCl. The heightened signal that converged at a single retention time for the quercetin precursor ions suggested that the release of free quercetin increased in tandem with the exposure time for the HCl treatment. In addition, the signals for the quercetin ions detected prior to 6.92 min declined significantly following the 24-hour treatment in comparison to the untreated, raw extract. This suggested that the hydrolysis of glycosides that were present in the raw extract correlated directly to the duration of the acid treatment.

The decline in the signal for quercetin ions detected in the HCl-treated samples occurred at the retention times associated with quercetin glycosides. This supported the identification of multiple glycosides (such as quercetin 3- β -D-glucoside, quercetin 3-galactoside, and quercitrin) during the analysis for the purified analyte. Consequently, the acid hydrolysis experiment provided confirming evidence that the fragmentation of quercetin glycosides accounted for the fact that there were multiple retention times for the quercetin detected during the extract analysis which deviated from the retention time (6.97 ± 0.02 min) defined for the commercial-grade quercetin. This result was consistent with the hypothesis that the quercetin ions detected early-on in the untreated, raw extract were the fragmenting ions of quercetin glycosides.

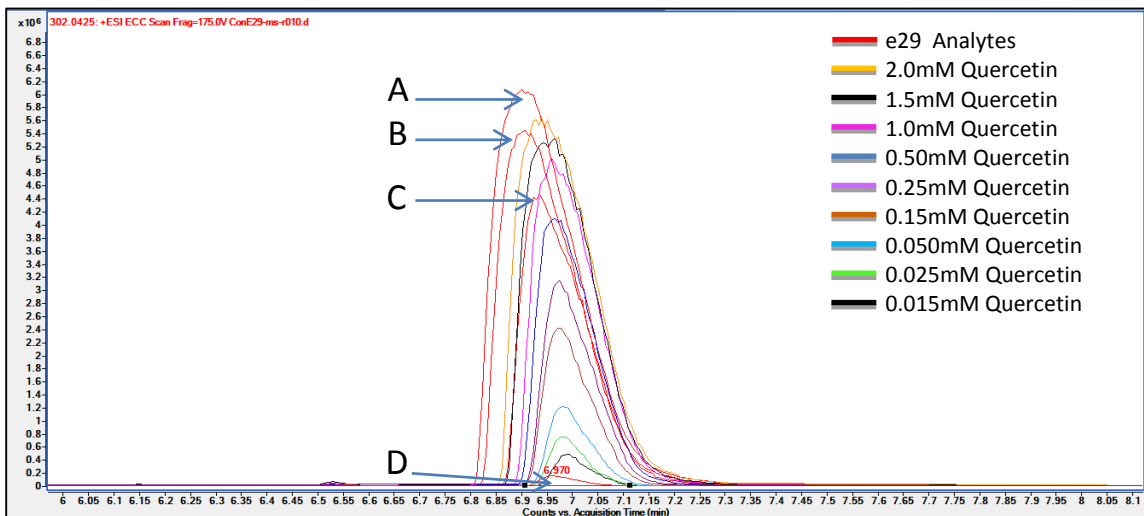


Figure 12. Extracted compound chromatogram for the quercetin standard curve integrated with ions of free quercetin detected in the HCl-treated and untreated e29 analytes.

In Figure 12, the combined extracted compound chromatogram (ECC) is shown for each concentration of the commercial-grade standard of quercetin that was analyzed to prepare the standard curve. In addition, the chromatographic peaks are shown for quercetin detected in each analyte that underwent acid treatments for the defined time periods (24h, 3h and 1h) as well as in the untreated raw extract are labeled (A, B, C, and D, respectively). Best-fit nonlinear regression analysis resulted in a standard curve illustrated in Appendix C. This regression analysis was based on the peak height (which measures the abundance of the selected precursor ions, related isotopic ions, and adduct ions detected within the same retention time window) for the quercetin ions detected at the concentration defined for each standard. Each concentration of the quercetin standard was prepared using serial dilution and analyzed via LC-QTOFMS. Following LC-QTOFMS analysis of the four aliquots of the raw extract (one untreated and three HCl-treated for different durations), the concentration of free quercetin was approximated based on the standard

curve. Only the concentrations for the peaks associated to free quercetin ions (m/z 303.0499±0.0005) within the retention time window of 6.95±0.03 min were approximated. The combined ECC (Figure 12) provided a visual comparison of the signal intensity for free quercetin resulting from each HCl-treated sample, versus the concentrations for the quercetin standards that were analyzed.

Following one hour of acid hydrolysis, the HCl-treated analyte C presented a signal for the free quercetin, which was approximated to a concentration of 0.88 mM of quercetin based on the standard curve ($R^2=0.997$). After three hours of acid hydrolysis, the analyte B presented an approximated concentration of 1.98 mM for the free quercetin in the sample. The analyte A (which underwent the 24-hour incubation with HCl) presented the most significant reduction of quercetin glycosides, which was signified by the amplified signal for the free quercetin ions when compared with the untreated and the other HCl-treated samples. Based on ECC (Figure 12), the analyte A presented a signal intensity of 4.99×10^6 counts for the free quercetin, which exceeded the upper limit of the standard curve (for which the maximum concentration of 2mM commercial-grade quercetin presented a signal of 4.64×10^6 counts). Given that the signal for the free quercetin in analyte A exceeded the scale for the standard curve, further LCMS analysis was performed with a diluted aliquot of analyte A. Following the quantification of the diluted aliquot, the concentration of free quercetin in analyte A was approximated to be 3.97 mM, based on the standard curve. Given that the concentration of free quercetin in analyte D was below the lower limit of the standard curve, the relative concentration (C_s) was determined to be 0.005 mM free quercetin, using the following equation:

$$C_s = C_x \frac{A_x}{A_s}$$

Here, the signal (A_x) for the quercetin in the analyte D and the signal (A_s) for the lowest concentration (C_x) of the quercetin standards was used to determine the C_s for the free quercetin detected in e29.

Overall, the steady increase in the concentration of free quercetin appeared to be a function of the duration for the acid hydrolysis, which also indicated that quercetin was hydrolyzed from the quercetin glycosides that were suspected to be present in the raw extract. The subsequent decline in the signal strength for the peaks of the suspected glycosides provided additional confirming evidence that glycosides of quercetin were accurately detected as hypothesized.

Enzyme kinetic characterization of quercetin with *Y. pestis*

As previously reported by Haymond et al. [8], the e29 exhibited potent inhibition of the enzyme-catalyzed oxidation of NADPH during dose-response assays with purified recombinant MEP synthase. The susceptibility of *Y. pestis* MEP synthase to commercial-grade quercetin was evaluated with a dose-response assay to determine half-maximal inhibitory concentration (IC₅₀) for quercetin and to evaluate its potency with respect to e29. The assays were performed in duplicate to examine the enzymatic response for MEP synthase in the presence of commercial-grade quercetin, relative to an uninhibited control.

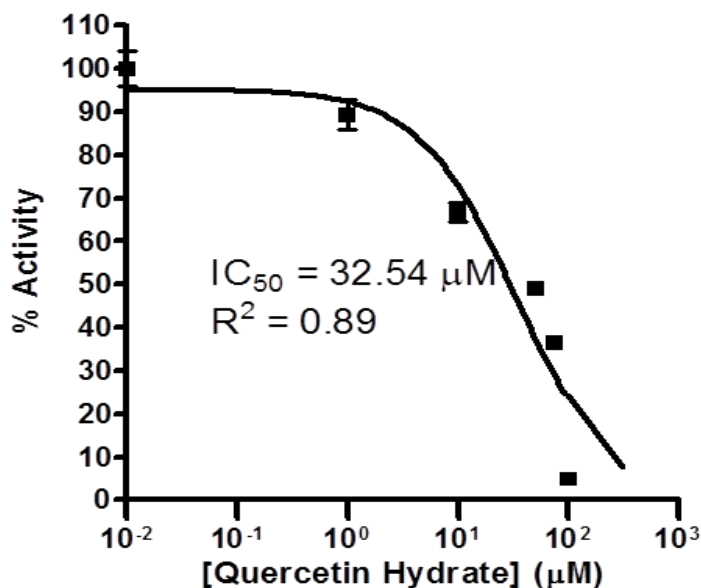


Figure 13. Kinetic characterization of quercetin with recombinant MEP synthase.

Figure 13 presents the dose response of recombinant MEP synthase during the enzyme assays with commercial-grade quercetin at various concentrations. The preincubation of MEP synthase with NADPH and quercetin was conducted concomitantly to form enzyme-inhibitor complexes. Then, DXP was added to activate the substrate-dependent oxidation of NADPH by MEP synthase, in order to reduce and isomerize DXP to form MEP [8]. As previously explained by Haymond et al. [8] for the characterization of e29, the assay samples were preincubated with NADPH to induce a conformational change required for the inhibitor and DXP. At the concentrations specified in Figure 13, the dose-response assay confirmed that quercetin significantly inhibited *Y. pestis* MEP synthase activity, comparable to inhibition in assays with e29. The commercial-grade quercetin exhibited an IC_{50} of 32.54 μ M ($R^2=0.89$), as shown in Figure 13.

Growth inhibition of *Y. pestis* with quercetin

The dose-response assay with MEP synthase (described above) further confirmed that the natural product quercetin was the lead inhibitor detected in e29. Next, the whole-cell growth

inhibition of liquid cultures of *Y. pestis* A1122 was examined over a 24 h period following treatments of cultures with serial dilutions of commercial-grade quercetin to determine bacteriostatic potency (see Figure 14). All growth assays were performed in duplicate at various concentrations of quercetin to determine the IC₅₀ for the inhibition of the bacterial cell growth.

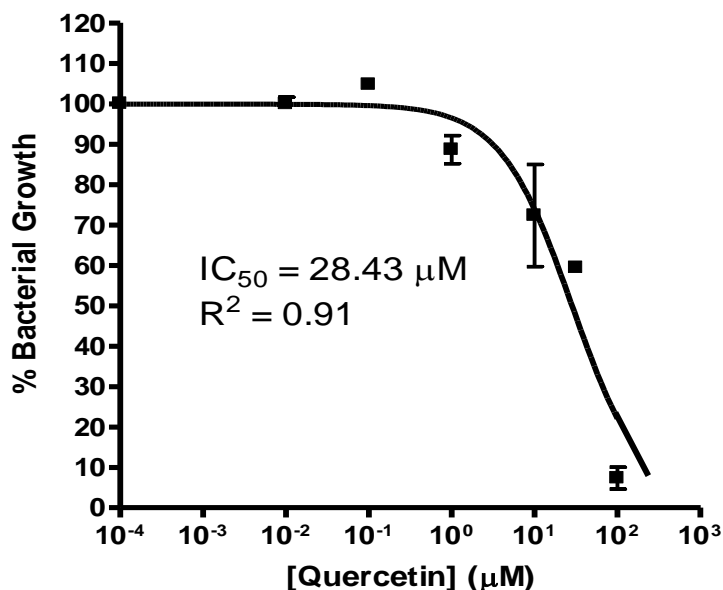


Figure 14. Bacterial growth inhibition assay of *Y. pestis* with quercetin.

As shown in Figure 14, the results of the growth inhibition assay indicated that commercial-grade quercetin presented an IC₅₀ of 28.43 µM (R²=0.91). As predicted, the commercial-grade quercetin presented bacteriostatic effects on the proliferation of *Y. pestis* cultures with a dose-dependent response that was similar to that of e29. During the whole-cell growth inhibition assay, the IC₅₀ for commercial-grade quercetin was also determined to be comparable to that of FR900098 (a well-characterized inhibitor of MEP synthase), which exhibited a slightly higher potency (IC₅₀ of 29.3 µM) against *Y. pestis* A1122 growth. Based on the

bacteriostatic potency during whole-cell growth inhibition assay, it was speculated that quercetin demonstrated cellular permeability for *Y. pestis* A1122 that was similar to that of FR900098.

Modality of inhibition by quercetin

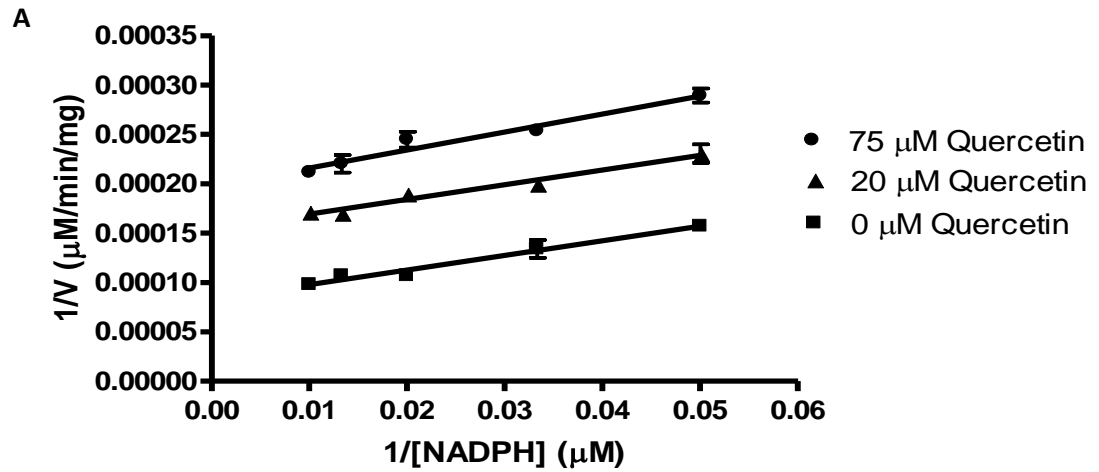
Given the potent, dose-dependent inhibition of recombinant *Y. pestis* MEP synthase by e29, the mechanism of action for e29 was characterized by Hammond et al. [8]. The data revealed that the active inhibitor in e29 was noncompetitive with respect to DXP (unlike FR90098 which is competitive with respect to DXP) and uncompetitive with respect to NADPH [8]. Given that all known MEP synthase inhibitors are competitive (i.e., selectively binding at the active site for the MEP synthase substrates), the inhibitory compound in e29 was determined to be a founding member of a novel class of antibiotics. Confirmatory analysis with purified, recombinant MEP synthase from *Mycobacterium tuberculosis* and *Francisella tularensis* (which are homologs of *Y. pestis* MEP synthase) were used to corroborate the allosteric mode of inhibition [8].

In order to validate quercetin as the identity for the active inhibitor in e29, the commercial-grade quercetin was expected to demonstrate the exact same mode of inhibition as the active inhibitor in e29. In order to examine the mode of inhibition with respect to each MEP synthase substrate (i.e., NADPH and DXP), MEP synthase was assayed with various concentrations of the selected substrate at fixed concentrations of the quercetin, while the concentration of the alternate MEP synthase substrate remained constant. During this analysis, a linear relationship was defined for the inhibition of MEP synthase by spectrometrically monitoring the rate of catalytic conversion of NADPH to NADP⁺ by MEP synthase under each experimental condition.

A Lineweaver-Burk plot was used to define these relationships and determine the mode of inhibitor interactions [31, 43]. The linear relationships are defined for the plot based on the Michaelis-Menten equation [31, 43]:

$$\frac{1}{v} = \frac{K_m}{V_{max}[S]} + \frac{1}{V_{max}}$$

In a Lineweaver-Burk plot, the x-axis represents the inverse concentration of substrates ($1/[S]$) and the y-axis represents the inverse of enzymatic rate of conversion ($1/v$) [31, 43]. The x-intercept indicates the relative negative inverse for substrate concentration at half the maximum reaction rate ($-1/K_m$) [31]. The y-intercept is the inverse of maximum catalytic activity ($1/V_{max}$) for the enzyme under the given experimental conditions, and the slope is defined as K_m/V_{max} [31, 43].



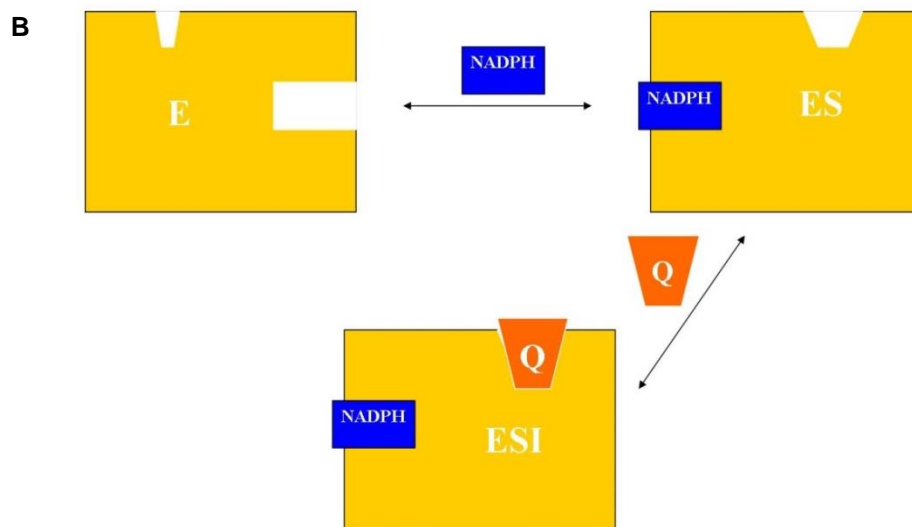


Figure 15. Modality of inhibition for quercetin with respect to NADPH.

The mode of inhibition for quercetin with respect to NADPH (Figure 15) was determined while maintaining the concentration of the recombinant MEP synthase and the standard assay buffer solution as constants. Three fixed concentrations (0, 20, and 75 microliters) of quercetin were compared at various concentrations of NADPH in the assay with MEP synthase. The maximum reaction rate (V_{max}) decreased when the concentration of quercetin increased. The K_m for NADPH declined in response to an increase in the quercetin concentration. The Lineweaver-Burk plot (Figure 15A) revealed that quercetin was uncompetitive with respect to NADPH. Figure 15B illustrates the mechanism of uncompetitive inhibition for the inhibitor (i.e., quercetin), as described by Copeland [31]. Consequently, the results suggested that the enzyme-NADPH complex must form prior to the binding of the quercetin. This outcome was consistent with previous findings by Haymond et al. [8] for the e29 inhibitor with respect to NADPH.

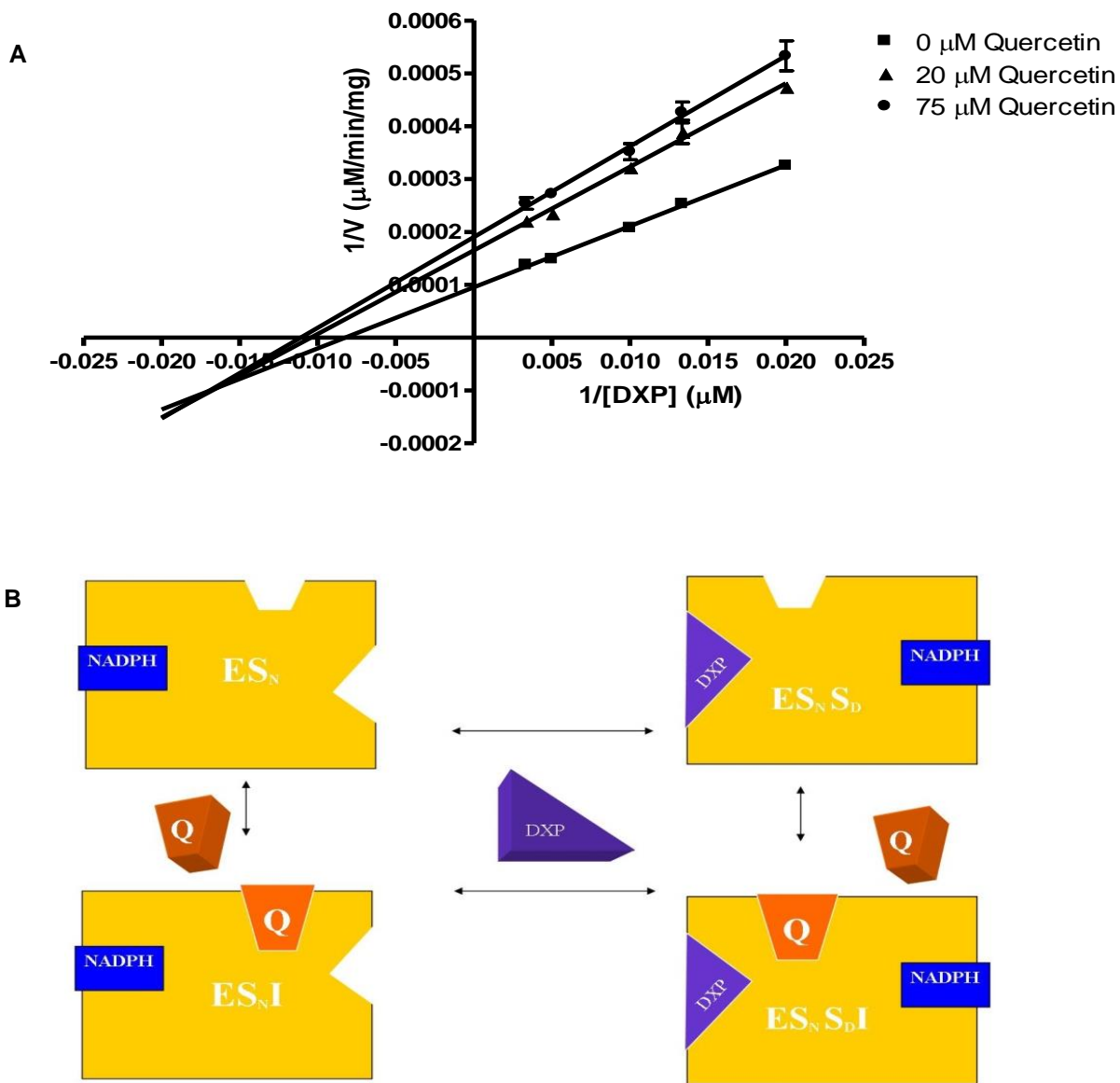


Figure 16. Modality of inhibition for quercetin with respect to DXP.

The mode of inhibition for quercetin with respect to DXP (Figure 16A) was determined while maintaining the concentration of the recombinant MEP synthase and the standard assay buffer solution as constant variables. The enzyme activity for MEP synthase was assayed using

three fixed concentrations of quercetin while the DXP concentration was gradually increased. The K_m for DXP remained constant when the concentration of quercetin was increased. In the interim, the maximum reaction rate, V_{max} , declined when the concentration of quercetin was increased. Thus, MEP synthase activity continued to decline as the concentration of quercetin increased, despite increases in the concentration of DXP. This outcome was exactly the same for e29, as determined during previous analysis by Hammond et al. [8]. Given that the K_m remained constant, DXP continued to bind at a normal rate regardless of an increase in either the concentration of the commercial-grade quercetin or e29. Given that V_{max} declined while K_m remained constant with respect to an uninhibited control, it was concluded that quercetin was a noncompetitive inhibitor with respect to DXP. Thus, quercetin was able to inhibit catalytic conversion of DXP to MEP, irrespective of the formation of an enzyme-DXP complex. Figure 16B illustrates the mechanism of noncompetitive inhibition for the inhibitor (i.e., quercetin), as demonstrated by Copeland [31].

Based on the fact that quercetin caused inhibition without competition for either the active binding site for NADPH or DXP, it was concluded that quercetin is a founding member of a novel class of allosteric inhibitors that obstruct the catalytic activity of MEP synthase. The findings of the Lineweaver-Burk analysis for NADPH and DXP met the expectations for the inhibitory compound found in e29. The allosteric mechanism of inhibition is an essential attribute for quercetin that signifies the presence of an alternative binding site for the development and optimization of future novel class MEP synthase inhibitors.

Quercetin passed the battery of tests that were implemented to validate the identity of the lead active inhibitor in e29. Each experiment of this study provided confirming evidence that quercetin was in fact the lead novel inhibitor detected in e29. The outcome of the identification and characterization of the novel inhibitor also provided a means to validate the methodology that this pharmacognosic research applied to selectively identify a lead inhibitor from the complex metabolome of the raw extract.

CONCLUSION

In this research, MEP synthase provided a viable drug target to screen a proprietary natural product library for novel inhibitors. The growth inhibition assays with *Y. pestis* A1122 cell cultures also provided insight on the bacteriostatic quality of inhibitors present in the natural product extracts found in the in-house library. The use of MEP synthase for high-throughput molecular screening of natural products led to the discovery, identification, and validation of quercetin as a founding member for a novel class of inhibitors with a unique allosteric binding site on MEP synthase. Given that MEP synthase has genetic homologs in other MEP pathway-dependent pathogens, the discovery of the existence of a novel target site calls for further investigation. Overall, the outcome of the high-throughput molecular screening of the proprietary natural product library supported the viability of the bioprospecting approach used to discover novel antimicrobial agents.

The combination of optimized chromatography techniques, highly sensitive QTOF LCMS/MS technology, and comparative analysis involving reference spectra led to the identification of quercetin from the metabolome of *R. crispus* (e29). Subsequently, mechanistic assays supported the validation of quercetin as an allosteric effector of MEP synthase that was biosynthesized and detected in the metabolome of e29. The findings of the dose-response analysis indicated that quercetin presented an IC₅₀ of 28.43 μM in growth inhibition assays with *Y. pestis* cultures *in vitro* and IC₅₀ of 32.54 μM in the enzyme kinetic assays with recombinant *Y. pestis* MEP synthase. Overall, growth inhibition and enzyme kinetic assays performed during the validation process provided a case for further research involving protein crystallography, in order to elucidate the binding site associated to quercetin. The elucidation of the allosteric binding site could facilitate the development of a novel array of broad-spectrum inhibitors that are not

susceptible to the upregulation and subsequent accumulation of substrate pools, which can diminish the effectiveness of competitive inhibitors [8, 16, 17]. In addition, further research to evaluate the potency of quercetin in assays with biosafety level 2 (BSL2) pathogens (such as *Francisella tularensis novicida*) is currently underway. Other research involving active transporter mutants and other etiological pathogens (e.g., *Mycobacterium tuberculosis* and *Plasmodium falciparum*) that present a biological threat could be used to provide additional evidence for the broad-spectrum implications of using quercetin as model for ongoing bioprospecting and the development of analogs that target the same allosteric binding site which interferes with MEP synthase activity.

In addition to investigating the broad-spectrum inhibition qualities of quercetin, it may be beneficial to explore ways of improving its potential as a novel drug candidate. Studies have shown that quercetin has low oral bioavailability in absence of its glycone, which enhances gastrointestinal absorption [44, 45]. Thus, the additional examination of the pharmacophoric properties of quercetin is necessary for comprehensive lead optimization as part of the drug discovery process. The key in lead optimization is to find the optimal point for improving target affinity, lipophilicity, and bioavailability while maintaining a balance for ADMET (absorption, distribution, metabolism, excretion and toxicity) properties [36, 44].

The apparent similarities between the active compound in e29 and quercetin did not rule out the possibility of a synergistic, combination effect involving other bioactive metabolites within the e29 metabolome. It is important to note that the structures of the prospective flavonoids that were identified in the purified analyte are very similar. A review of supporting literature confirmed that these flavonoids were biosynthesized within the same phenylpropanoid or malonic acid pathways [25, 46, 47]. However, the detection of similar metabolites in the purified analyte that presented low affinity for the MEP synthase target can be anticipated to occur in tandem with the lead inhibitor following purification, due to their similarities in structure. It remains possible that the metabolome from the e29 consisted of biologically active metabolites that present a

synergistic effect with the lead inhibitor, while not showing any inhibition when assayed with the MEP synthase target alone [25]. Likewise, there is a potential for little or no biological effect by other metabolites that compete for the same binding site. This could explain why multiple compounds (quercetin 3- β -D-glucoside, quercetin 3-galactoside, quercitrin, \pm catechin, and epicatechin) with a similar structure and functional groups as quercetin were detected as potential candidates following purification while several even presented minor inhibitory effects during enzyme kinetic assays.

The protocols used in this study presented an effective means to detect and identify novel, potent inhibitors of MEP synthase using natural products. Advanced analytical technology and techniques (such as highly-sensitive spectrometry, chromatography, and purification) were utilized to support the discovery, identification, and validation of inhibitor hits from the proprietary natural product library. In recent natural product research, advancements in techniques and technology have enhanced the evaluation of the physiological effects on organisms and their metabolic machinery [25]. Similar to the present study, related advancements have driven new discoveries in antimicrobial drug targets and treatments [25].

When pharmaceutical research and development (R&D) investments shifted away from pharmacognosy in the 1990s, there was a decline in the discovery of novel classes of antibiotics [14]. In recent years, the emergence of drug-resistant pathogens (some classified as bioterrorism threats) has emphasized the urgent need for new drug discovery and novel treatments [14, 25, 48]. Bioprospecting of natural product libraries presents validated potential for the immediate discovery of novel drug treatments that have not yet been subjected to evolving microbial resistance to the commercially available treatments. Meanwhile, more than 60% of the drugs currently on the market are derived from the exploration of only 10% of the plant species [25, 26, 28]. Given that there are over 300,000 plant species alone, there is great potential for the ongoing discovery of novel and diverse drug candidates through the molecular screening of natural product libraries [25].

APPENDICES

APPENDIX A

Selective Secondary Screening of Natural Product Extracts by Growth Inhibition Assay with *Y. pestis*.

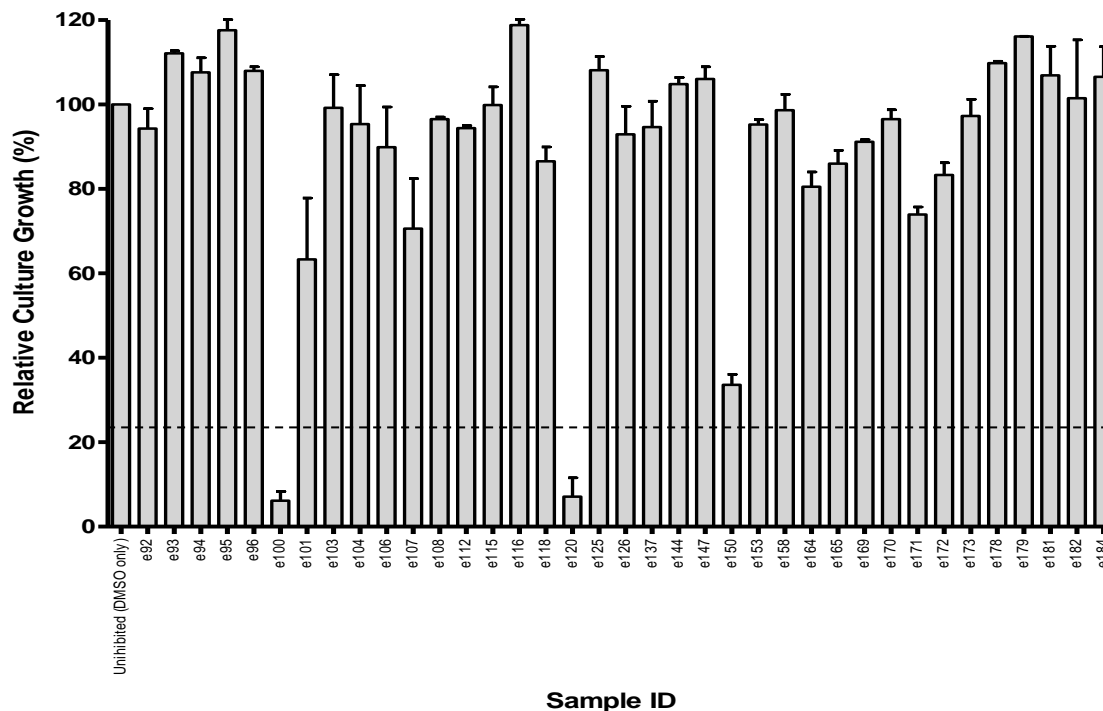


Figure 17. Selective molecular screening with *Y. pestis* bacterial growth inhibition screening.

Secondary molecular screenings were performed using growth inhibition assays with *Y. pestis* A112 to screen select extracts from the natural product library for the presence of active compounds with bacteriostatic properties. As shown in Figure 17, this selective library screening only included natural product extracts that were pre-determined to have antimicrobial activity through literary review of prior research. Each assay was performed in duplicate and an uninhibited culture was prepared in absence of raw extract to serve as a reference in order to measure the percent growth. The bacteriostatic quality of the majority of these natural product extracts was relatively low compared to the uninhibited *Y. pestis* cultures. While three hit extracts (e100, e120, and e150) demonstrated apparent growth inhibition (>70%), each presented less than 50% inhibition when screened with purified MEP synthase.

APPENDIX B

Tandem mass spectra: difference spectral analysis for potential lead compound with METLIN database references [30] at collision energies 10 V, 20 V, and 40 V.

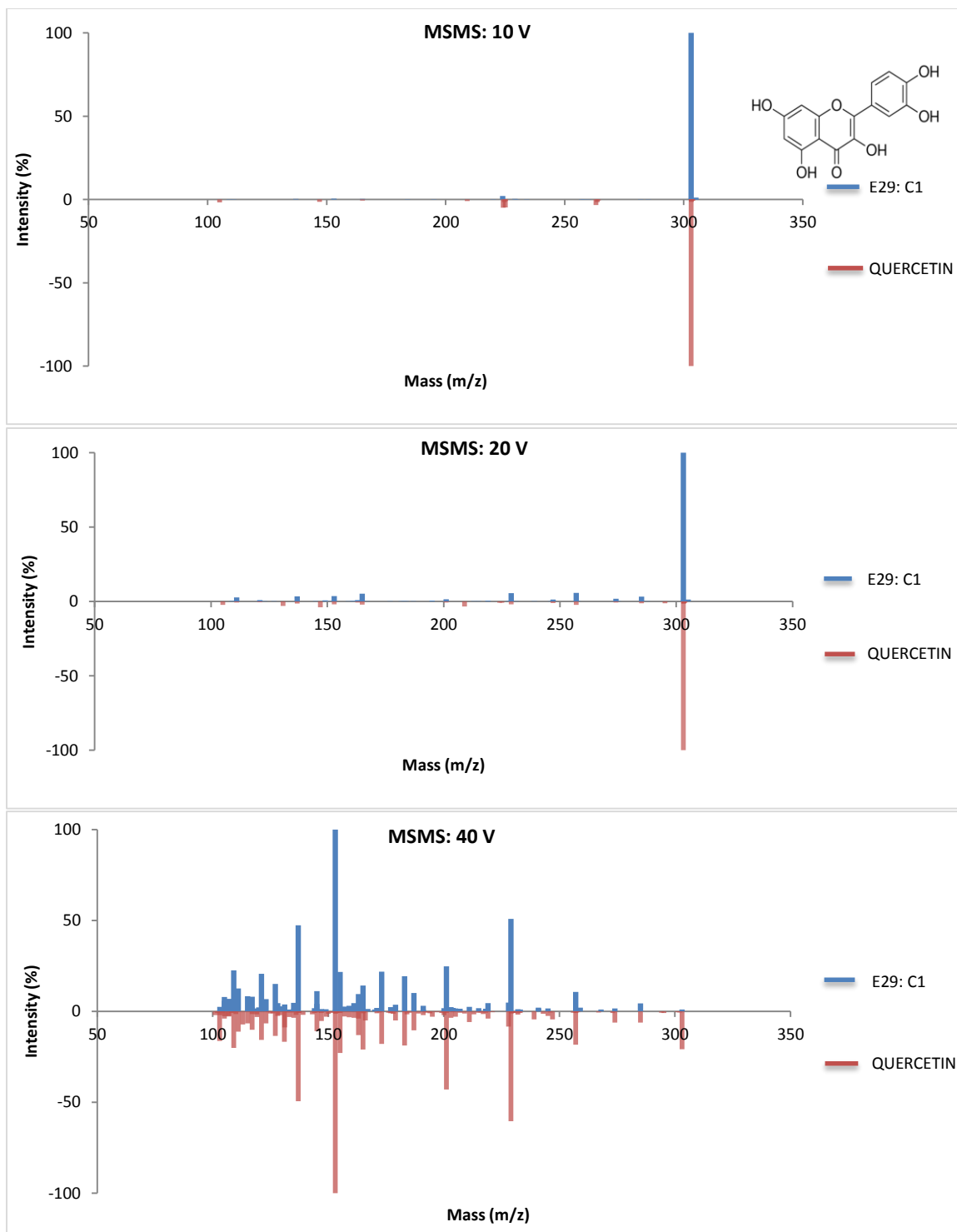


Figure 18. MS/MS difference spectral analysis for quercetin in extract 29 and quercetin reference.

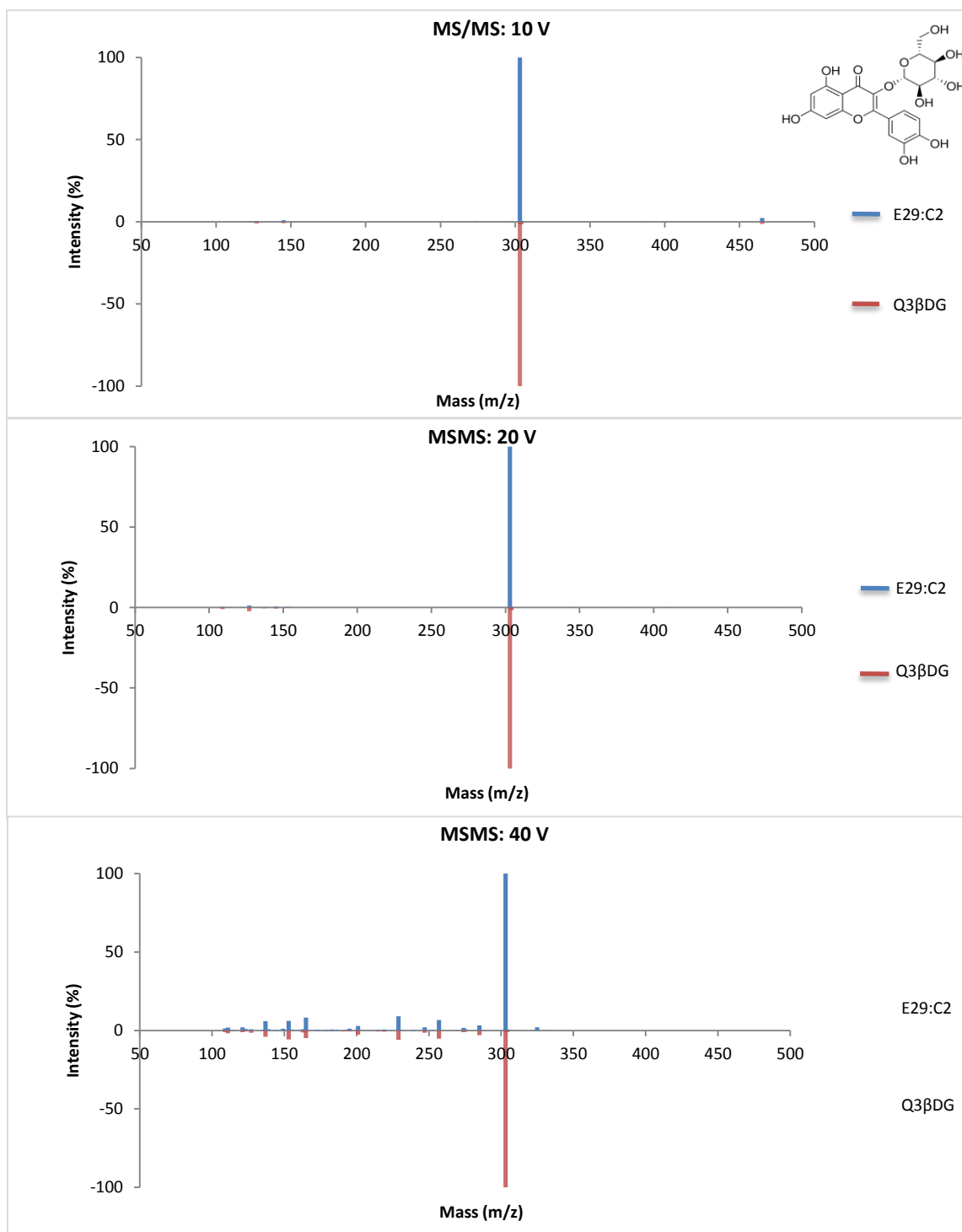


Figure 19. MS/MS difference spectral analysis for extract 29 potential and quercetin 3-β-D-glucoside reference.

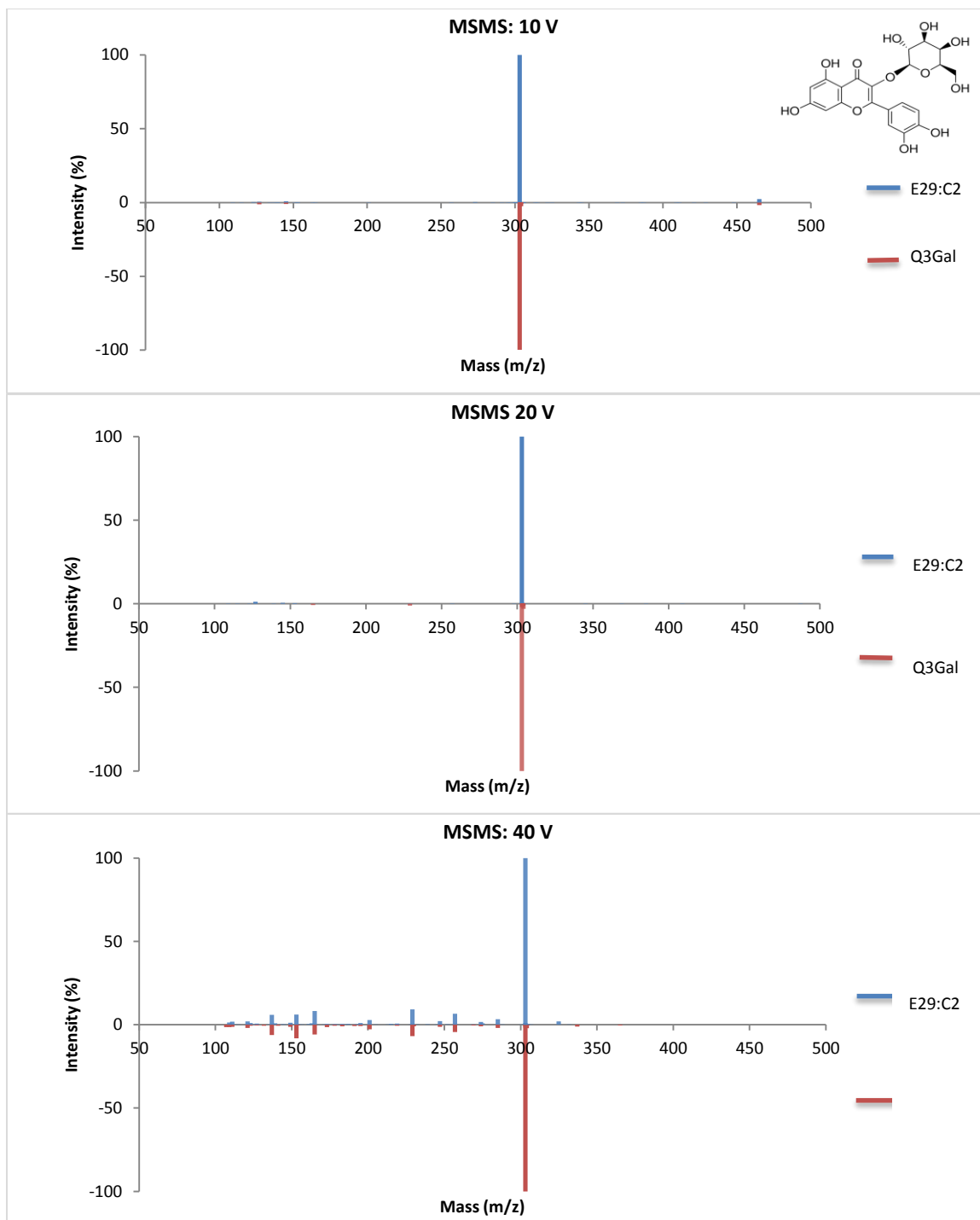


Figure 20. MS/MS difference spectral analysis for extract 29 potential and quercetin 3-galactoside reference.

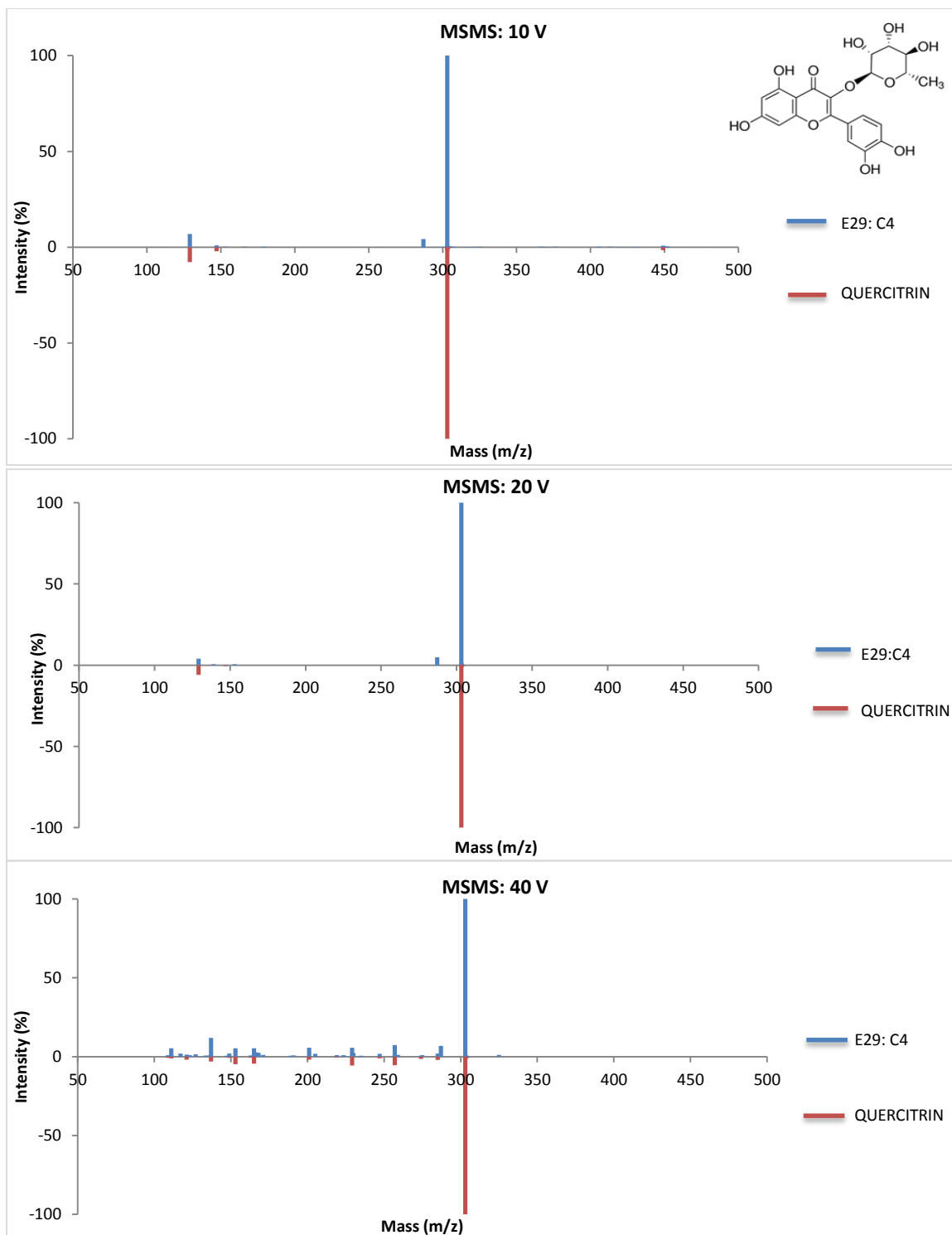


Figure 21. MS/MS difference spectral analysis for extract 29 potential and quercitrin reference.

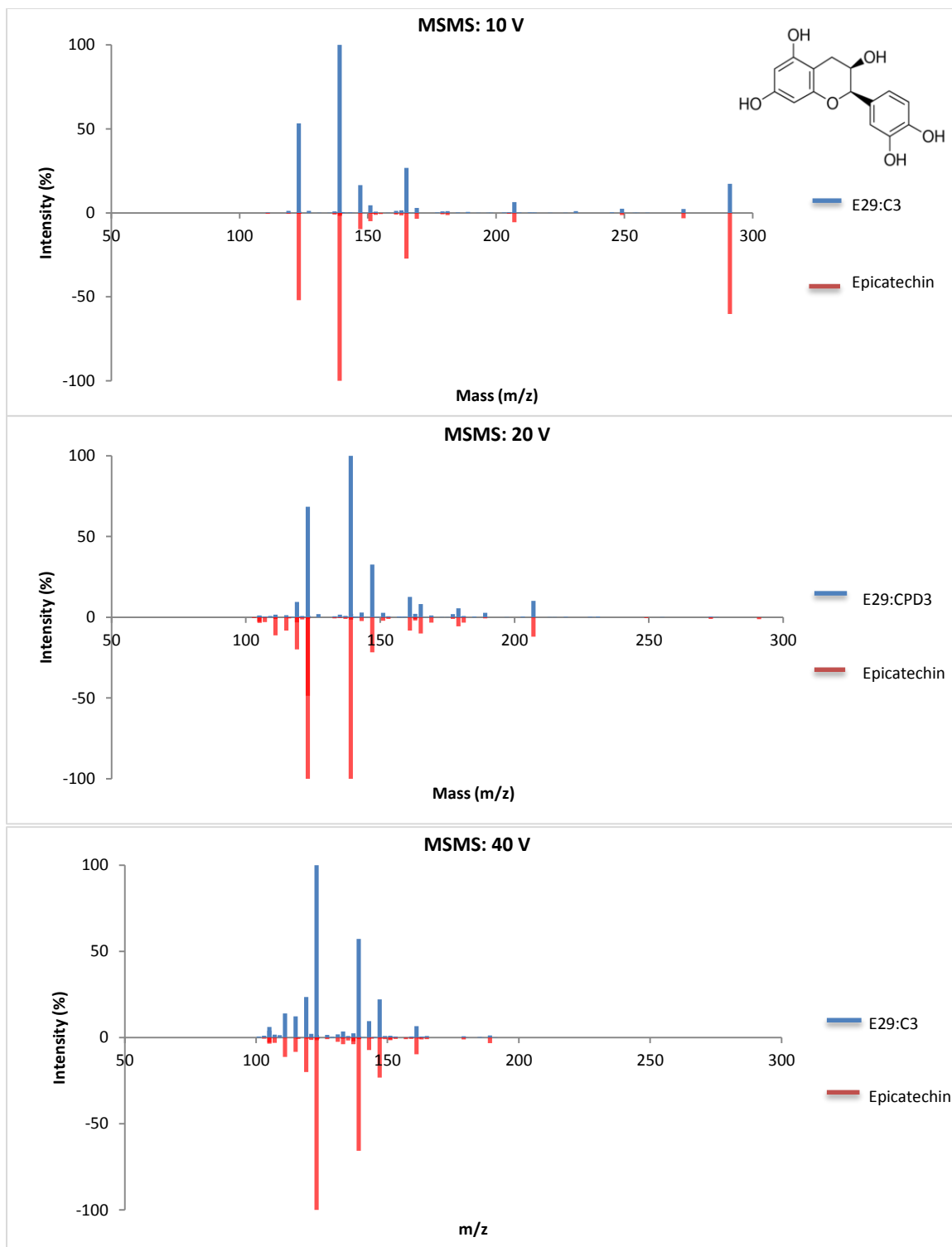


Figure 22. MS/MS difference spectral analysis for extract 29 potential and epicatechin reference.

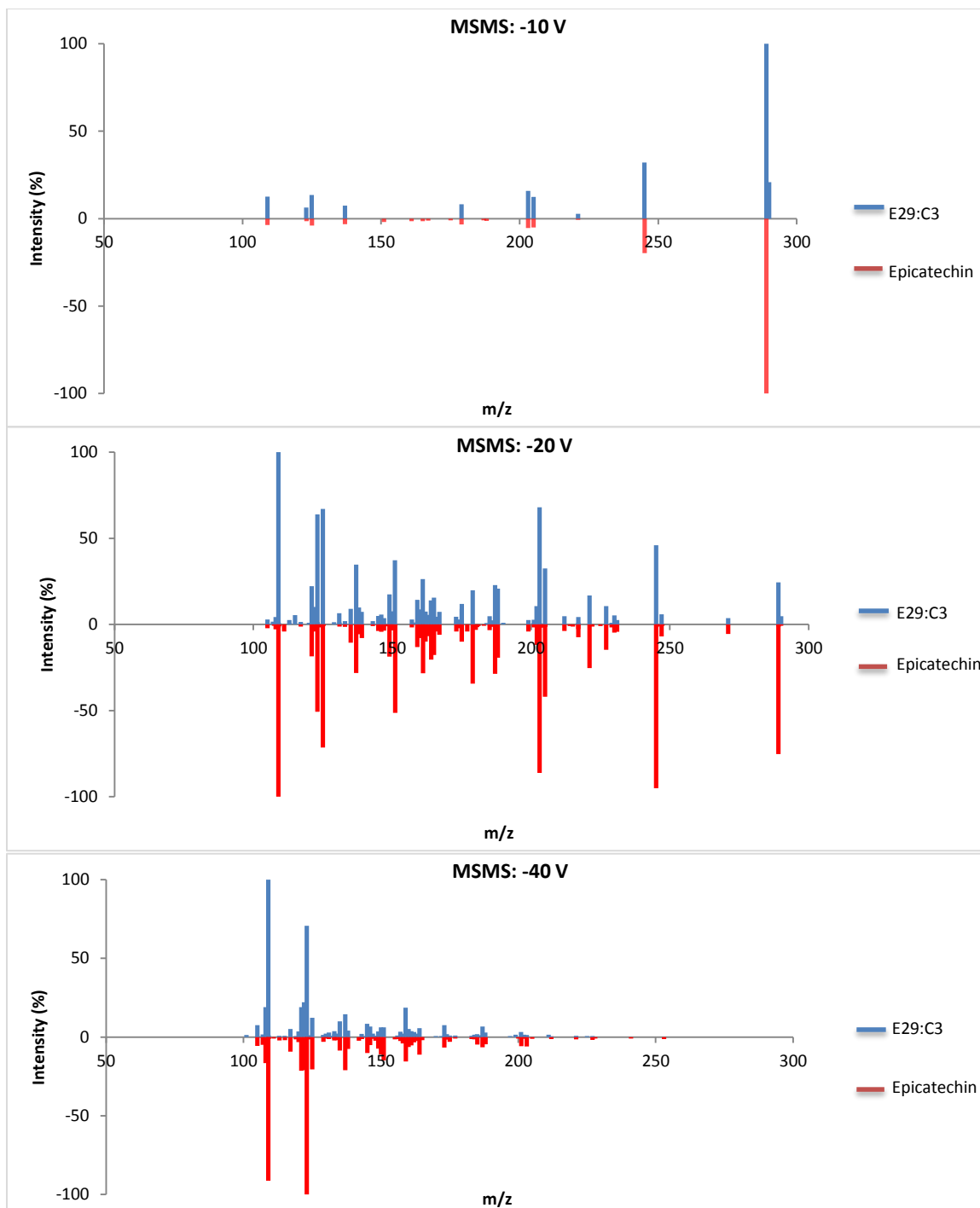


Figure 23. MS/MS difference spectral analysis for extract 29 potential and epicatechin reference (Negative Mode).

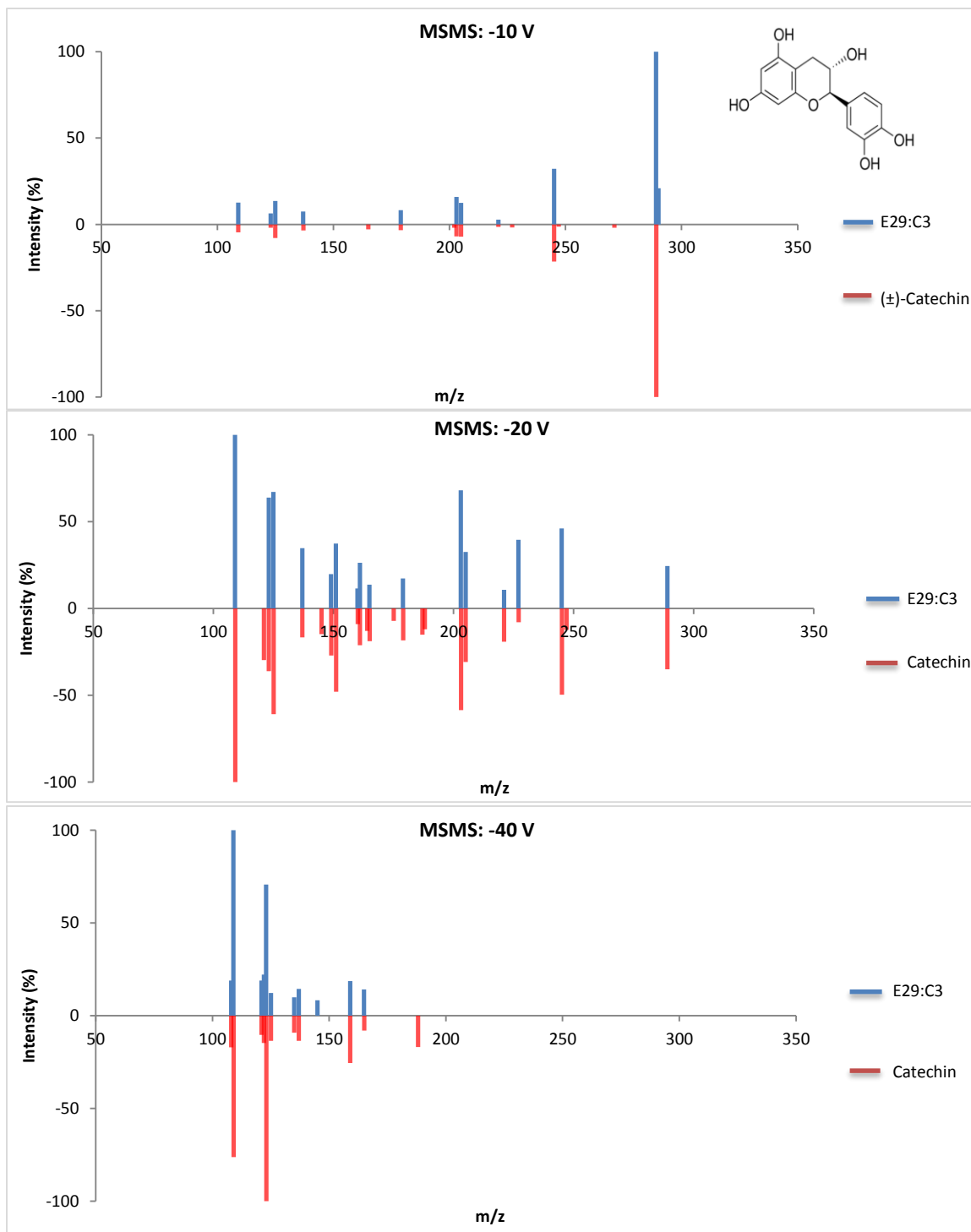


Figure 24. MS/MS difference spectral analysis for extract 29 potential and (±)-catechin reference (Negative Mode).

APPENDIX C

Standard curve using nonlinear regression for quercetin standard solutions.

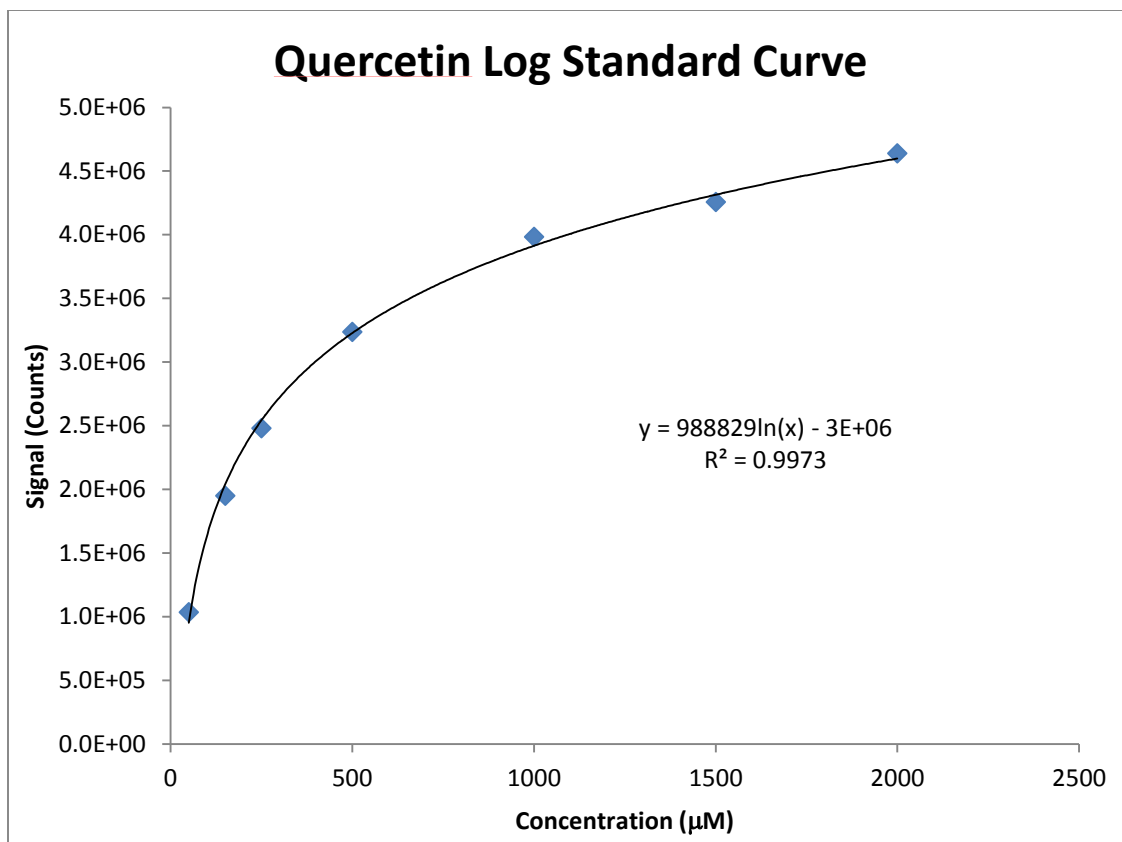


Figure 25. Standard curve for quercetin reference standards.

APPENDIX D

Procedure for preparation of MSMS difference spectral results for empirical and visual comparative analysis of metabolite fingerprint vs. MS/MS spectra database references.

I. To acquire empirical data:

A. From MassHunter Qualitative Analysis Software B.06.00 SP2

1. Open Data File associated to data of interest
2. Check "Load Data Results"
3. From toolbar, select NAVIGATION VIEW
4. Goto METHOD EXPLORER /FIND COMPOUNDS/ Find by Molecular Feature
(for MS only)
 - i. ION SPECIES tab
 - Allow: +H, +Na, +NH₄, -H, +Cl, H₂O
 - ii. CHARGE STATE tab
 - PEAK SPACING TOLERANCE: 0.0025 m/z, plus 5.0
 - ISOTOPE MODEL: Common organic molecules
 - CHARGE STATE:
 - a. Maximum of 2
 - b. Treat unassigned charge as singly-charged
 - iii. COMPOUND FILTERS tab
 - HEIGHT: Absolute >= 5000 counts
 - COMPOUND QUALITY: Score >= 82
 - iv. EXTRACTION tab
 - EXTRACTION ALGORITHM: Target small molecule
(chromatographic)
 - v. MASS FILTERS tab
 - FILTER MASS LIST: 7 ppm
 - a. Select "Exclude these mass(es) from drop menu
 - SOURCE OF MASSES:

- a. Paste m/z detected in Blank Sample (Standard Reaction Matrix)
 - b. Include m/z with a height or abundance above 10K
- vi. RESULTS tab, check as follows:
 - Delete previous compounds
 - Extract EIC, ECC, raw spectrum, MFE spectrum
5. To assign IDs to m/z refer to Section III
6. Highlight data in COMPOUND LIST, select Export to excel or CSV format
7. In Excel, sort data by m/z to perform empirical comparative analysis
 - i. Grey out (to eliminate) m/z from analyte that are equivalent to those detected in negative control (blank)
 - ii. On separate excel sheet copy only the m/z that are unique to analyte
 - iii. Rank according to abundance or height
8. Goto METHOD EXPLORER /FIND COMPOUNDS/ Find by Auto MSMS (for MSMS)
 - i. Select PROCESSING tab, enter as follows:
 - RETENTION TIME WINDOW: 1.0 min
 - POSITIVE MS/MS TIC THRESHOLD: 1000 (abundance counts)
 - NEGATIVE MS/MS TIC THRESHOLD: 1000 (abundance counts)
 - MASS MATCH TOLERANCE: 0.0010 m/z
 - Uncheck "Limit to the largest"
 - Uncheck "Filter results by fragment"
 - In PERSISTENT BACKGROUND COMPOUNDS window
 - a. REMOVE IF THERE ARE MORE THAN: 5
 - b. EXCEPT WHEN TIC EXCEEDS: 10000

- ii. Select EXCLUDED MASSES tab, enter as follows:
 - Enter the m/z detected in Blank Sample or Base Reaction Mix
 - Symmetric (ppm): 10.0 (lowest possible)
 - iii. Select RESULTS tab, check as follows:
 - Delete Previous Compounds
 - Extract ECC, MS & MS/MS
 - Extract separate MS/MS spectrum per collision energy
9. Save method and click  to begin processing
10. Once data processing is complete, select COMPOUND DETAILS VIEW
11. Goto VIEW tab, select COMPOUND FRAGMENT RESULTS to see MS/MS for select ion
 - i. If no spectrum appears, select NAVIGATOR VIEW tab
 - Highlight compound in COMPOUND LIST
 - Right-click and select "Extract Complete Result Set"
 - Repeat steps 6-7
12. In COMPOUND DETAILS VIEW mode,
 - i. Select COMPOUND LIST window and highlight compound of interest
 - ii. Select METHOD EXPLORER/REPORTS/Compound Report
 - Check "Show compound table", "Show MS peak table", "Show predicted isotope macthc table", "Show MS/MS spectrum" and "Show MS/MS peak table"
 - iii. Save method and click  to begin processing
 - iv. In PRINT COMPOUND REPORT window, check as follows
 - Only Highlighted Results
 - Save report as Excel file

- At specified directory: Assign folder
 - Auto-generate new report file name
13. Locate EXCEL file for [dataset name and collision energy]MSMS_CompoundReport.
 14. Open and scroll down to MS/MS SPECTRUM PEAK LIST to see fragment ion m/z and their abundances.

B. If using METLIN Database for Reference data

1. Search database for a specific compound, chemical formula or m/z
2. Tolerance should be 3-5ppm to improve accuracy and reduce the number of hits
 - i. Choose a compound of interests
 - ii. Goto column for MSMS, select VIEW
 - For spectrum, select Collision Energy that corresponds to sample acquisition parameters to view corresponding spectrum
3. Right-click on spectrum, select VIEW SOURCE
4. Scroll down to script that corresponds to Collision Energy
5. Highlight script for all the collision energies used in the experiment
 - i. Right-click and Copy
6. Open WORD document
 - i. Select NEW/CREATE
 - ii. Paste data
7. Clean data and eliminate script
 - i. Highlight repetitive scripts
 - ii. Goto EDITING, select REPLACE
 - Click FIND WHAT bar, paste unwanted script
 - Click REPLACE WITH bar, hit spacebar twice (2x)

- a. Select REPLACE ALL
 8. Once complete, only the X (m/z) and Y (%Intensity) data should remain
 9. Goto INSERT/TABLE/Draw Table
 - i. Fit all X-data into one column and Y-data in separate column
 - ii. Highlight and copy to EXCEL document.
-

II. To prepare difference spectral charts in EXCEL:

B. Setup two columns for spectral data in XY order:

1st. X-axis = m/z for fragment ions

2nd. Y-axis = intensity for each fragment

- Determined signal Intensity:
 - Define base peak, or most abundant fragment, abundance (BPA) cell
 - Calculate percent abundance for each fragment ion abundance (FIA) cell:
 - Use formula: $=(\text{FIA cell\#/BPA cell\#}) * 100$.

C. Setup for two spectra chart

1. Highlight one XY-data set
2. Select INSERT/SCATTER
3. Right-click on one data point and CHART TOOLS menu will appear above taskbar
4. Under CHART TOOLS, select LAYOUT
 - i. Then select ERROR BARS/ More Error Bars Options

- If the message “Add Error Bars?” appears, specify for which data set
 - ii. When VERTICAL ERROR BARS menu appear, enter as follows:
 - Direction: minus
 - End style: No cap
 - Error Amount: 100%
 - Line Color: Solid
 - Line Sylte: Width: 2 pt
 - Close
- 5. Goto upper left-hand selection window (under "File; Home")
 - i. Click for dropdown menu
 - ii. Select series "Data set name" X Error Bar
- 6. Under slection window, click FORMAT SELECTION menu
 - i. When VERTICAL ERROR BARS window appear, enter as follows:
 - Horizontal Error Bar
 - Direction: Both
 - End Style: No Cap
 - Error Amount/Fixed Value: 0
 - Line Color: No line
 - Close
- 7. Right-click on chart and choose “Select Data” from menu
 - i. When SELECT DATA SOURCE window appears:
 - Select ADD
 - Manual select data that corresponds to Empirical Reference MSMS data set

- Select OK
8. Data points will appear on graph, then repeat steps 3-6 for new data
 9. Data will be overlaid in chart.

D. To create the mirror plane for difference spectral analysis:

1. Select and copy INTENSITY % data for Reference only (typically the least complex of the two sets, thus fewer data point)
2. Right-click on 1st cell in following column
 - i. Goto PASTE OPTIONS in menu
 - ii. Select VALUES (123) option
3. Click first cell of original INTENSITY% data
 - i. Enter formula: = -{#cell for copied INTENSITY% data}
 - ii. Double-click or drag-down copy bar
4. Mirror plane with reference data will appear
5. Format according to preferences.

III. To get a general idea of the potential identities, chemical formulas and related scores for the compounds that are detected:

- A. From MassHunter Qualitative Analysis Software B.06.00 SP2
 1. Open Data File for data of interest for MS only
 2. Check "Load Data Results"
 3. From toolbar, select NAVIGATION VIEW
 4. Goto METHOD EXPLORER /FIND COMPOUNDS by FORMULA/
 5. Select "Find by Formula –Options", and enter as follows:
 - i. NEGATIVE or POSITIVE IONS: Select according

- ii. FORMULA SOURCE: "Database/Library"
 - If installed, choose
"C:\MassHunter\PCDL\Metlin_Metabolites_AM_PCDL.cdb"
 - iii. VALUES TO MATCH: "Mass and Retention time(retention time optional)
 - iv. FORMULA MATCHING:
 - Masses: +/- 5.00 ppm
 - Retention times: +/- 1.00 minute
 - Possible m/z: +/-10.0
 - Uncheck "Limit EIC extraction range"
 - v. FRAGMENT CONFIRMATION: Uncheck "Confirm with fragment ions"
 - vi. RESULTS:
 - Check "Delete previous compounds"
 - Uncheck all under CHROMATOGRAMS and SPECTRA
 - a. Save time, memory and file size
6. Upon complete, compounds and potential identities will be available in COMPOUND LIST window

B. To combine MSMS compounds with MS IDs

1. Open file for MSMS data after completing FIND COMPOUND/Auto MSM
2. Select COMPOUND LIST window and click column for m/z
 - i. All data should arrange according to m/z for MSMS and MS compounds
3. Highlight all, right-click and select EXPORT
 - i. In EXPORT window, select as follows:
 - FILE TYPE: "Data as Excel file"
 - EXPORT CONTENTS: "Only highlighted rows"
 - EXPORT DESTINATION: "Specified file" and select location

4. Retreat excel file in location to begin empirical comparative analysis.

REFERENCES

1. Riedel, S. (2005) Plague: from natural disease to bioterrorism. *Proc (Bayl Univ Med Cent)*. 18(2): 116–124.
2. Urich, S.; Chalcraft, L.; Schriefer, M.; Yockey, B.; Petersen, J. Lack of Antimicrobial Resistance in *Yersinia pestis* Isolates from 17 Countries in the Americas, Africa, and Asia.(2012) *Antimicrob Agents Chemother*. 56(1): 555–558.
3. Perry, R.D.; Fetherston, J.D. (1997) *Y. pestis* —Etiologic agent of plague. *Clin. Microbiol. Rev.* 10(1): 35.
4. Wheelis, M. (1999) Biological Warfare before 1914. In *Biological and Toxin Weapons: Research, Development and Use from the Middle Ages to 1945*. Geissler, E. & Moon, J.E., Ed. Oxford University Press: London.
5. Harris, S.H. (1994) *Factories of death: Japanese biological warfare 1932–45 and the American cover-up*. Routledge: New York.
6. Lockwood, J. (2008) *Six-legged soldiers: Using insects as weapons of war*. Oxford University Press: New York.
7. Alibek, K.; Handelman, S. (1999) *Biohazard: The chilling true story of the largest covert biological weapons program in the world—Told from the inside by the man who ran it*. Random House: New York.
8. Haymond, A.; Johnny C.; Dowdy, T.; Schweibenz, B.; Villarroel, K.; Young, R.; Mantooth, C.; Patel, T.; Bases, J.; San Jose, G.; Jackson, E. Dowd, C.; Couch, R. (2014) Kinetic characterization and allosteric inhibition of the *Yersinia pestis* 1-Deoxy-D-Xylulose 5-Phosphate Reductoisomerase (MEP Synthase). *PLoS ONE*. 9(8): e106243.
9. Centers for Disease Control. Bioterrorism Agents and Diseases. (2014) Agent List (Online) <http://www.bt.cdc.gov/agent/agentlist-category.asp>
10. Li, B.; Yang, R. (2008) Interaction between *Yersinia pestis* and the Host Immune System. *Infect. Immun.* 76 (5): 1804-1811.
11. Salyers, A.; Whitt, D. (2002) *Bacterial pathogenesis: A molecular approach*, 2nd ed. ASM Press: Washington, D.C.
12. Rakin A.; Boolgakowa, E.; Heesemann, J. (1996) Structural and functional organization of the *Yersinia pestis* bacteriocin pesticin gene cluster. *Microbiology*. 142: 3415-3424.
13. Welch, T.; Fricke, W.; McDermott, P.; White, D.; Rosso, M-L.; Rasko, D.; Mammel, M.; Eppinger, M.; Rosovitz, M.; Wagner, D.; Rahalison, L.; LeClerc, J.; Hinshaw, J.; Lindler, L.; Cebula, T.; Carniel, E.; Ravel, J. (2007) Multiple Antimicrobial Resistance in Plague: An Emerging Public Health Risk. *PLoS ONE*. 2007, 2(3): e309.

14. Spellberg, B.; Guidos, R.; Gilbert, D.; Bradley, J.; Boucher, H.; Scheld, W.; Bartlett, J.; Edwards, J. (2008) The epidemic of antibiotic-resistant infections: A call to action for the medical community from the infectious diseases society of America. *Clin. Infect. Dis.* 46(2): 155–164.
15. Centers for Disease Control. (2014) Healthcare-associated Infections (HAIs): Data and Statistics. (Online) <http://www.cdc.gov/HAI/surveillance/index.html>
16. Uh, E.; Jackson, E.; San Jose, G.; Maddox, M.; Lee, R.; Lee, R.; Boshoff, H.; Dowd, C. (2011) Antibacterial and antitubercular activity of fosmidomycin and their lipophilic analogs. *Bioorg Med Chem Lett.* 21(23): 6973–6976.
17. McKenney, E.; Sargent, M.; Khan, H.; Uh, E.; Jackson, E.; San Jose, G.; Couch, R.; Dowd, C.; van Hoek, M. (2012) Lipophilic prodrugs of FR900098 are antimicrobial against *Francisella novicida* in vivo and in vitro and show GlpT independent efficacy. *PLoS One.* 7(10):e38167.
18. Cordoba, E.; Salmi, M.; León, P. (2009) Unravelling the regulatory mechanisms that modulate the MEP pathway in higher plants. *J. Exp. Bot.* 60(10): 2933-2943.
19. Nelson, D.; Cox, M. (2008) *Lehninger: Principles of biochemistry, 5th ed.* W.H. Freeman and Company: New York.
20. Hunter, W.N. (2007) The non-mevalonate pathway of isoprenoid precursor biosynthesis. *J. Biol. Chem.* 282: 21573–21577.
21. Eisenreich, W.; Bacher, A.; Arigoni, D.; Rohdich, F. (2004) Biosynthesis of isoprenoids via the non-mevalonate pathway. *Cell. Mol. Life Sci.* 61 (12): 1401–26.
22. Tsang, A. (2012) *Francisella tularensis* IspD: A target for novel antibiotics. MS Thesis. George Mason University: Fairfax, VA.
23. Cassera, M.; Merino, E.; Peres, V.; Kimura, E.; Wunderlich, G.; Katzin, A. (2007) Effect of fosmidomycin on metabolic and transcript profiles of the methylerythritol phosphate pathway in *Plasmodium falciparum*. *Mem Inst Oswaldo Cruz.* 102(3): 377–83.
24. Singh, N.; Chev e, G.; Avery, M.; McCurdy, C. (2007) Targeting the Methyl Erythritol Phosphate (MEP) Pathway for Novel Antimalarial, Antibacterial and Herbicidal Drug Discovery: Inhibition of 1-Deoxy-D-Xylulose-5-Phosphate Reductoisomerase (DXR) Enzyme. *Current Pharmaceutical Design.* 13: 1161-1177.
25. Cseke, L.; Kirakosyan, A.; Kaufman, P.; Warber, S.; Duke, J.; Briemann, H. (2006) *Natural products from plants*, 2nd ed. CRC Press: Florida.
26. Steenhuisen, J. (2007) Mother Nature, still a rich source of new drugs. *Reuters* (Online). <http://www.reuters.com/article/2007/03/20/environment-drugs-nature-dc-idUSN1624228920070320> (Accessed November 2013).

27. Davies, Julian. (2007) Microbes have the last word: A drastic re-evaluation of antimicrobial treatment is needed to overcome the threat of antibiotic-resistant bacteria. *European Molecular Biology Organization Reports*. 8(7): 616-621.
28. Elander, R.P. (2003) Industrial production of beta-lactam antibiotics. *Appl. Microbiol. Biotechnol.* 61(5-6): 385–392.
29. Levesque, F.; Seeberger, P. (2012) Continuous-flow synthesis of the anti-malaria drug artemisinin. *Angewandte Chemie Int. Ed.* 51: 1–5.
30. Scripps Center For Metabolomics. (2014) *METLIN: Metabolite and Tandem MS Database* (Online). http://metlin.scripps.edu/metabo_search_alt2.php
31. Copeland, R. (2005) *Evaluation of enzyme inhibitors in drug discovery. A guide for medicinal chemists and pharmacologists*. John Wiley & Sons, Inc.: New Jersey.
32. Agilent Technology, Inc. (2011) Agilent Time-of-Flight Mass Spectrometry: Technical Overview. (Online) <http://www.chem.agilent.com/Library/technicaloverviews/Public/5990-9207EN.pdf>
33. University of Kentucky. (2014) Summary of the characteristics of different mass analyzers. (Online). <http://www.chem.agilent.com/Library/technicaloverviews/Public/5990-9207EN.pdf>
34. Agilent Technologies, Inc. (2012) MassHunter METLIN Metabolite PCD/PCDL, Rev A. California.
35. Agilent Technology, Inc. (2012) Agilent 6200 series TOF and 6500 series Q-TOF LC/MS system: Concepts guide, Rev. A. California.
36. Hann, M.; Keserü, G. (2012) Finding the sweet spot: The role of nature and nurture in medicinal chemistry. *Nature Reviews Drug Discovery*. 11: 356–365.
37. Walle, T.; Browning, A.; Steed, L.; Reed, S.; Walle, U. (2005) Flavonoid glucosides are hydrolyzed and thus activated in the oral cavity in humans. *J. Nutr.* 135(1): 48–52.
38. Zhang, C.; Liu, G.; Hu, F. (2012) Hydrolysis of flavonoid glycosides by propolis β -glycosidase. *Natural Product Research: Formerly Natural Product Letters*. 26(3): 270–273.
39. Tan, K.; Tesar, C.; Wilton, R.; Keigher, L.; Babnigg, G.; Joachimiak, A. (2010) Novel α -glucosidase from human gut microbiome: substrate specificities and their switch. *FASEB J.* 24(10): 3939–3949.
40. Henrissat, B.; Davies, G. (1995) Structures and mechanisms of glycosyl hydrolases. *Structure*. 3(9): 853–859.

41. Wang, J.; Zhao, L.; Sun, G.; Liang, Y.; Wu, F.; Chen, Z.; Cui, S. (2011) A comparison of acidic and enzymatic hydrolysis of rutin. *African Journal of Biotechnology*. 10(8): 1460–1466.
42. Khoddami, A.; Wilkes, M.; Roberts, T. (2013) Techniques for Analysis of Plant Phenolic Compounds. *Molecules*. 18: 2328-2375.
43. Worthington Biochemical Corp. (2014) Intro to enzymes: Substrate concentration. (Online). <http://www.worthington-biochem.com/introbiochem/substrateconc.html>
44. Singh, S.; Konwar, B. (2012) Molecular docking studies of quercetin and its analogues against human inducible nitric oxide synthase. *SpringerPlus*. 1:69.
45. Cermak, R.; Landgraf, S.; Wolfram, S. (2003) The bioavailability of quercetin in pigs depends on the glycoside moiety and on dietary factors. *J Nutr*. 133(9): 2802-7.
46. Akagi, T., Ikegami, A., Suzuki, Y.; Yoshida, J.; Yamada, M; Sato, A.; Yonemori, K. (2009) Expression balances of structural genes in shikimate and flavonoid biosynthesis cause a difference in proanthocyanidin accumulation in persimmon (*Diospyros kaki* Thunb.) fruit. *Planta*. 230(5): 899–915.
47. Winkel-Shirley, B. (2001) Flavonoid biosynthesis. A colorful model for genetics, biochemistry, cell biology, and biotechnology. *Plant Physiol*. 126: 485–493.
48. Mitsuhashi, S. (1977) *R Factor: Drug resistant plasmid*. University Park Press: Maryland.

BIOGRAPHY

Tyrone Dowdy graduated from Open High School, Richmond, Virginia, in 1994 and received his bachelor degree in Biology and Psychology from George Mason University (GMU) in 2000. He was employed as social worker, supervisor, and program manager providing family-based therapeutic services (i.e. counseling, developmental treatment, educational support, and advocacy) for children with mental health, autism and other developmental disorders. He also worked in the biotech industry as a lab technician for two years. He returned to GMU in 2012 to pursue his master's degree in chemistry with a concentration in biochemistry. This provided an opportunity to gain one and a half years' combined experience as a graduate research assistant on Dr. Robin Couch's research team and as a graduate lecturer for the Chemistry and Biochemistry Department. Following his experience at GMU, he continued working as a research associate at the Metabolomics Shared Resource lab in the Department of Oncology at Georgetown University.